primary hepatocytes[6] and cirrhotic rat liver[7] through mammalian target of rapamycin (mTOR) signaling, a central regulator of protein synthesis, by sensing nutrient conditions.[8] Thus, peripheral amino acid composition is closely related to signaling pathways in the liver.

In addition to metabolic aspects, recent reports have elucidated new functional roles for mTOR in the IFN signaling pathway. Targeted disruptions of tuberous sclerosis 2 and eukaryotic translation initiation factor 4E binding protein 1, which both inhibit mTOR complex 1 (mTORC1) signaling, substantially enhanced IFN-alfa–dependent antiviral responses.[9,10] Therefore, mTORC1 signaling might be involved in the antiviral response as well as in metabolic processes. However, these issues have not yet been addressed in terms of IFN treatment for CH-C. In the present study, therefore, we evaluated the clinical relevance of the nutritional state of the liver, as estimated by the plasma Fischer's ratio, on Peg-IFN and RBV combination therapy. We also evaluated antiviral signaling induced by BCAA using an in vitro HCV replication system.

Materials and Methods

Patients

A total of 168 patients with CH-C at the Graduate School of Medicine at Kanazawa University Hospital (Kanazawa, Japan) and its related hospitals in Japan (Table 1, Supplementary Table 1) were evaluated in the present study. The clinical characteristics of these patients have been described previously.[4] All patients were administered Peg-IFN-alfa 2b (Schering-Plough K.K., Tokyo, Japan) and RBV combination therapy for 48 weeks. The definition of the treatment response was as follows: sustained viral response (SVR), clearance of HCV viremia 24 weeks after the cessation of therapy; transient response (TR), no detectable HCV viremia at the cessation of therapy but relapse during the follow-up period; and no response (NR). Genetic variation of the IL-28B polymorphism at rs8099917 was evaluated in all patients using TaqMan Pre-Designed SNP Genotyping Assays (Applied Biosystems, Carlsbad, CA) as described previously.[4] Gene expression profiling in the liver was performed in 91 patients using the Affymetrix Human 133 Plus 2.0 microarray chip (Affymetrix, Santa Clara, CA) as described previously (Supplementary Table 1).[4]

Plasma Amino Acid Analysis

Amino acid concentrations in plasma samples were measured by high-performance liquid chromatography–electrospray ionization–mass spectrometry, followed by derivatization.[11] Detailed experimental procedures are described in the Supplementary Materials and Methods section.

Culture Medium

Huh-7 and Huh-7.5 cells (kindly provided by Professor C. M. Rice, Rockefeller University, New York, NY) were maintained in Dulbecco's modified Eagle medium (DMEM; Gibco BRL, Gaithersburg, MD) containing 10% fetal bovine serum and 1% penicillin/streptomycin (normal medium). Amino acid-free medium (ZERO medium) was prepared by mixing 5.81 g nutrition-free DMEM (Nacalai Tesque, Kyoto, Japan), 1.85 g $NaHCO_3$, 1 g glucose, and 0.5 mL 1M (mol/L) sodium pyruvate in 500 mL Milli-Q water, then sterilizing with a 0.22-μm filter (Millipore, Billerica, MA). Low amino acid media (×1/5, ×1/10, ×1/30, and ×1/100 DMEM) were prepared by diluting ×1 DMEM with ZERO medium. Powdered BCAA (leucine-isoleucine-valine, 2:1:1.2) (Ajinomoto Pharma, Tokyo, Japan) was freshly dissolved with distilled water at 100 mmol/L, then applied to cultured medium at 2 mmol/L, 4 mmol/L, or 8 mmol/L.

Western Blotting and Immunofluorescence Staining

A total of 1.5×10^5 Huh-7 cells were seeded in normal medium 24 hours before performing the experiments. The medium was changed to low-amino-acid medium and maintained for up to 24 hours. Western blotting was performed as previously described.[12] Cells were washed in phosphate-buffered saline (PBS) and lysed in RIPA buffer containing complete Protease Inhibitor Cocktail and PhosSTOP (Roche Applied Science, Indianapolis, IN). The membranes were blocked in Blocking One-P (Nacalai Tesque). The antibodies used for Western blotting are summarized in the Supplementary Materials and Methods section.

For immunofluorescence staining, cells were fixed with 4% paraformaldehyde in PBS, then permeabilized with 0.1% Triton-X 100 in PBS. The primary anti-forkhead box O (Foxo)3a antibody (Abcam, Cambridge, MA) was used at a final concentration of 2 μg/mL in PBS containing 2% fetal bovine serum at 4°C for 16 hours. Incubation with the Alexa Fluor 488–conjugated secondary antibody (Invitrogen, Carlsbad, CA) at a 500-fold dilution in PBS containing 3% fetal bovine serum antibody was performed for 4 hours, and cells were stained with Hoechst 33258 to visualize nuclear DNA (Vector Laboratories, Burlingame, CA).

Quantitative Real-Time Detection Polymerase Chain Reaction

A total of 1.5×10^5 Huh-7 cells were seeded in normal medium 24 hours before performing the experiments. The medium was changed to low-amino-acid medium, to which IFN-alfa and/or BCAA was added, and maintained for 24 hours. Rapamycin treatment (100 nmol/L) was performed for 30 minutes in normal medium before a medium change. RNA was isolated using TriPure isolation reagent (Roche Applied Science), and complementary DNA (cDNA) was synthesized using the High Capacity cDNA reverse transcription kit (Applied Biosystems, Carlsbad, CA). Real-time detection polymerase chain reaction (PCR) was performed using the 7500 Real-Time PCR System (Applied Biosystems) and Power SYBR Green PCR Master Mix (Applied Biosystems) containing specific primers according to the manufacturer's

Table 1. Comparison of Clinical Factors Between Patients With and Without NR

Clinical category	SVR+TR	NR	Univariate *P* value	Multivariate odds (95% CI)	Multivariate *P* value
Patients, n	125	43		—	
Age and sex					
Age, y	57 (30–72)	56 (30–73)	.927	—	
Sex, male vs female	68 vs 57	24 vs 19	.872	—	
Liver histology					
F stage (F1–2 vs F3–4)	95 vs 30	20 vs 23	.001	6.35 (2.02–23.7)	.001
A grade (A0–1 vs A2–3)	68 vs 57	19 vs 24	.248	—	
Host gene factors					
IL-28B (TT vs TG/GG)[a]	109 vs 12	12 vs 31	<.001	19.7 (5.74–82.7)	<.001
ISGs (Mx, IFI44, IFIT1), (<3.5 vs ≥3.5)	103 vs 22	12 vs 31	<.001	5.26 (1.65–17.6)	.005
Metabolic factors					
BMI, kg/m^2	23.2 (16.3–34.7)	23.4 (19.5–40.6)	.439	—	
TG, mg/dL	98 (30–323)	116 (45–276)	.058	—	
T-Chol, mg/dL	167 (90–237)	160 (81–214)	.680	—	
LDL-Chol, mg/dL	82 (36–134)	73 (29–123)	.019	—	
HDL-Chol, mg/dL	42 (20–71)	47 (18–82)	.098	—	
FBS, mg/dL	94 (60–291)	96 (67–196)	.139	—	
Insulin, μU/mL	6.6 (0.7–23.7)	6.8 (2–23.7)	.039	—	
HOMA-IR	1.2 (0.3–11.7)	1.2 (0.4–7.2)	.697	—	
Fischer ratio	2.3 (1.5–3.3)	2.1 (1.5–2.8)	.005	8.91 (1.62–55.6)	.011
Other laboratory parameters					
AST level, IU/L	46 (18–258)	64 (21–283)	.017	—	
ALT level, IU/L	60 (16–376)	82 (18–345)	.052	—	
γ-GTP level, IU/L	36 (4–367)	75 (26–392)	<.001	—	
WBC, /mm^3	4800 (2100–11100)	4800 (2500–8200)	.551	—	
Hb level, g/dL	14 (9.3–16.6)	14.4 (11.2–17.2)	.099	—	
PLT, ×104/mm^3	15.7 (7–39.4)	15.2 (7.6–27.8)	.378	—	
Viral factors					
ISDR mutations ≤1 vs ≥2	80 vs 44	34 vs 9	.070	4.12 (1.25–15.9)	.019
HCV-RNA, KIU/mL	2300 (126–5000)	1930 (140–5000)	.725	—	
Treatment factors					
Total dose administered					
Peg-IFN, μg	3840 (960–7200)	3840 (1920–2880)	.916	—	
RBV, g	202 (134–336)	202 (36–336)	.531	—	
Achieved administration rate					
Peg-IFN, %					
≥80%	84	28	.975	—	
<80%	42	14			
RBV (%)					
≥80%	76	24	.745	—	
<80%	50	18			
Achievement of EVR	101/125 (81%)	0/43 (0%)	<.001	—	

BMI, body mass index; CI, confidence interval; FBS, fasting blood sugar; γ-GTP, gamma-glutamyl transpeptidase; Hb, hemoglobin; HDL-chol, high density lipoprotein cholesterol; LDL-chol, low density lipoprotein cholesterol; PLT, platelets; T-chol, total cholesterol; TG, triglycerides; WBC, leukocytes.

[a]IL-28B SNP at rs8099917.

instructions. The primer sequence for real-time detection PCR is given in the Supplementary Materials and Methods section. HCV RNA was detected as described previously[12] and expression was standardized to that of glyceraldehyde-3-phosphate dehydrogenase.

Reporter Assay

Construction of the interferon stimulated response element (ISRE)-luc reporter plasmid and Socs3-luc or Socs3 (FoxO binding element mutant [FBEmut])-luc reporter plasmids is described in the Supplementary Materials and Methods section.

Huh-7 cells were transfected with the ISRE-luc reporter plasmid 24 hours before IFN-alfa treatment. Cells were treated with IFN-alfa (0 or 100 U/mL) and BCAA (2 mmol/L) in low-amino-acid media. After 24 hours, luciferase activities were measured using the Dual Luciferase assay system (Promega, Madison, WI). For Socs3 promoter activities, Huh-7 cells were transfected with Socs3-luc or Socs3 (FBEmut)-luc reporter plasmids together with the Foxo3a expression plasmid, and luciferase activities were measured after 24 hours. Values were normalized to the luciferase activity of the co-transfected pGL4.75 Renilla luciferase-expressing plasmid (Promega).

Knockdown Experiments

Huh-7 cells were transfected with Ctrl (Stealth RNAi Negative Control Low GC Duplex #2; Invitrogen) or

targets (regulatory associated protein of mTOR [Raptor] and Foxo3a) (Supplementary Materials and Methods) small interfering RNA (siRNA) using Lipofectamine RNAiMAX reagent (Invitrogen) according to the manufacturer's instructions. After 48 hours, cells were cultured in normal or low-amino-acid media for a further 24 hours. The knockdown effect was confirmed by Western blotting.

Chromatin Immunoprecipitation Assay

Detailed experimental procedures are described in the Supplementary Materials and Methods section.

HCV Replication Analysis

pH77S3 is an improved version of pH77S, a plasmid containing the full-length sequence of the genotype 1a H77 strain of HCV with 5 cell culture–adaptive mutations that promote its replication in Huh-7 hepatoma cells.[13] pH77S.3/Gaussia luciferase (GLuc)2A is a related construct in which the GLuc sequence, fused to the 2A autocatalytic protease of foot-and-mouth virus RNA, was inserted in-frame between p7 and NS2[14] (Supplementary Materials and Methods). A signal sequence in GLuc directs its secretion into cell culture media, allowing real-time, dynamic measurements of GLuc expression to be performed without the need for cell lysis.

A 10-μg aliquot of synthetic RNA transcribed from pH77S.3/GLuc2A was used for electroporation. Cells were pulsed at 260 V and 950 μF using the Gene Pulser II apparatus (Bio-Rad Laboratories, Hercules, CA) and plated in fresh normal medium for 12 hours to recover. Cell medium was changed to ×1 DMEM without serum for 8 hours, then changed to low-amino-acid medium containing 0–8 mmol/L BCAA for a further 24 hours. Cells and culture medium were collected and used for GLuc assays, real-time detection PCR, and Western blotting. The number of viable cells was determined by a (3-[4,5-dimethylthiazol-2-yl]-5-[3-carboxymethoxyphenyl]-2-[4-sulfophenyl] -2H-tetrazolium, inner salt) assay (Promega).

Continuously JFH-1–infecting Huh-7 cells were obtained by the infection of Huh-7 cells with JFH-1 cell culture-derived HCV at a multiplicity of infection of 0.01. Cells were maintained in normal medium by passaging every 3–4 days for approximately 6 months. About 20%–30% of the cells consistently were positive for HCV core protein (Supplementary Figure 4). Culture medium of JFH-1–infecting Huh-7 cells was changed to the low-amino-acid medium containing 0–8 mmol/L BCAA for 24 hours. Cells then were collected and used for assays.

Statistical Analysis

Results are expressed as mean ± standard deviation. Significance was tested by 1-way analysis of variance with the Bonferroni method, and differences were considered statistically significant at a P value of less than .05.

Results

Fischer's Ratio as a Predictive Factor for Treatment Response

The clinical characteristics of patients who received Peg-IFN and RBV combination therapy are shown in Table 1 and Supplementary Table 1, and explanations of these characteristics have been described previously.[4] All patients were infected with HCV genotype 1b and had a high viral load (>100 IU/mL). We compared patients with SVR + TR against those with NR, as assessed by the overall plausibility of treatment response groups using Fisher's C statistic as previously described.[4] We included data on the IL-28B polymorphism and plasma amino acid composition (aminogram).

Univariate regression analysis showed that no single amino acid was associated significantly with treatment response; however, using Fischer's ratio, the BCAA (Ile+Leu+Val)/aromatic amino acids (Phe+Tyr) ratio was associated significantly with treatment response (P = .005) (Table 1). Of the 121 patients with IL-28B major type, SVR, TR, and NR were observed in 53%, 37%, and 10%, respectively, and among 33 patients with IL-28B minor type, SVR, TR, and NR were observed in 15%, 17%, and 68%, respectively (P < .001) (data not shown). Fischer's ratio of SVR, TR, and NR was 2.35 ± 0.38, 2.30 ± 0.29, and 2.10 ± 0.31, respectively (P < .015) (data not shown).

We selected IL-28B polymorphism, hepatic ISG expression, fibrosis stage, HCV RNA, interferon sensitivity determining region mutation, and Fischer's ratio as factors for multivariate analysis. Multivariate analysis revealed that the minor type of IL-28B polymorphism (TG or GG at rs8099917) (odds ratio, 19.7; P < .001), advanced fibrosis stage of the liver (F3–4) (odds ratio, 6.35; P = .001), high hepatic ISGs (≧3.5) (odds ratio, 5.26; P = .005), low Fischer's ratio (continuous range, 1.5–3.3) (unit odds, 8.91; P = .011), and presence of ISDR mutation (≦1) (odds ratio, 4.12; P = .019) independently contributed to NR (Table 1).

The distribution of the Fischer's ratio according to fibrosis stage is shown in Supplementary Figure 1. The ratio decreased significantly in advanced fibrosis stage (F3–4) compared with early fibrosis stage (F1). No significant association between major or minor type of IL-28B polymorphism and different fibrosis stages of the liver was observed (Supplementary Figure 1*A*). In early fibrosis (F1–2) (Supplementary Figure 1*B*), 90% (80 of 89) of SVR+TR cases had the major type of IL-28B polymorphism, and 94% (16 of 17) of NR cases had the minor type. However, in the advanced fibrosis stage of the liver (F3–4) (Supplementary Figure 1*C*), 85% (23 of 27) of SVR+TR cases had the major type of IL-28B polymorphism and 50% (10 of 20) of NR cases had the minor type. Thus, in advanced fibrosis stages, factors other than the IL-28B polymorphism appear to contribute to NR. Interestingly, the Fischer's ratio was significantly lower in NR patients than SVR+TR pa-

tients in the advanced fibrosis stage of the liver. Therefore, Fischer's ratio could be an important predictor for NR that is independent of IL-28B polymorphism and histologic stage of the liver.

Fischer's Ratio and mTORC1 Signaling in CH-C Livers

Hepatic gene expression in 91 of 168 patients (Supplementary Table 1) was obtained using Affymetrix genechip analysis as described previously.[4] To examine the relationship between the plasma Fischer's ratio and mTORC1 signaling in the liver we evaluated the expression of key regulatory genes related to mTORC1 signaling. We found that expression of branched chain amino-acid transaminase 1 (BCAT1), an important catalytic enzyme of BCAA, was significantly negatively correlated with Fischer's ratio (Figure 1*A*). This indicates that the plasma Fischer's ratio is regulated in the liver as well as in peripheral muscle. Interestingly, the expression of c-myc, a positive regulator of BCAT1 (Figure 1C),[15] was correlated negatively with the Fischer's ratio (Figure 1*B*). The expression of PDCD4, a negative transcriptional target of ribosomal p70 S6 protein kinase (S6K), downstream of mTORC1, was correlated significantly with BCAT1 (Figure 1*D* and *E*). Thus, in CH-C livers, BCAT1 is induced with progressive liver disease and mTORC1 signaling is repressed, a process that might involve c-myc. Fischer's ratio of the plasma therefore can be seen to reflect mTORC1 signaling in the liver.

Impaired IFN Signaling in Huh-7 Cells Grown in Low-Amino-Acid Medium

Recent reports have shown the functional relevance of mTOR on IFN signaling and antiviral responses.[9,10] To evaluate IFN-alfa signaling and the mTOR pathway, we used Huh-7 cells grown in different amino acid conditions (×1 DMEM, ×1/5 DMEM, ×1/30 DMEM, and ×1/100 DMEM). The phosphorylated forms of mTOR (p-mTOR) and S6K (pS6K), an important downstream regulator of mTORC1 signaling, were decreased substantially in ×1/30 DMEM and ×1/100 DMEM (Figure 2*A*). Interestingly, the expression of the phosphorylated form of signal transducer and activator of transcription 1 (pSTAT1), an essential transducer of type 1 IFN signaling, also was decreased in these conditions (Figure 2*A*). Similarly, the expression of p-mTOR and pSTAT1 was repressed significantly in CH-C livers with a low Fischer's ratio compared with those with a high Fischer's ratio (Supplementary Figure 2, Supplementary Table 2).

To examine whether decreased pSTAT1 expression might be owing to repressed mTORC1 signaling, we knocked down the expression of Raptor, a specific subunit of mTORC1. We achieved more than 50% knockdown of Raptor by specific siRNA (Figure 2*B*). Under these conditions, the expression of p-mTOR and pSK6 were repressed, which is consistent with previous reports.[16] The expression of pSTAT1 also was repressed after Raptor knockdown (Figure 2*B*).

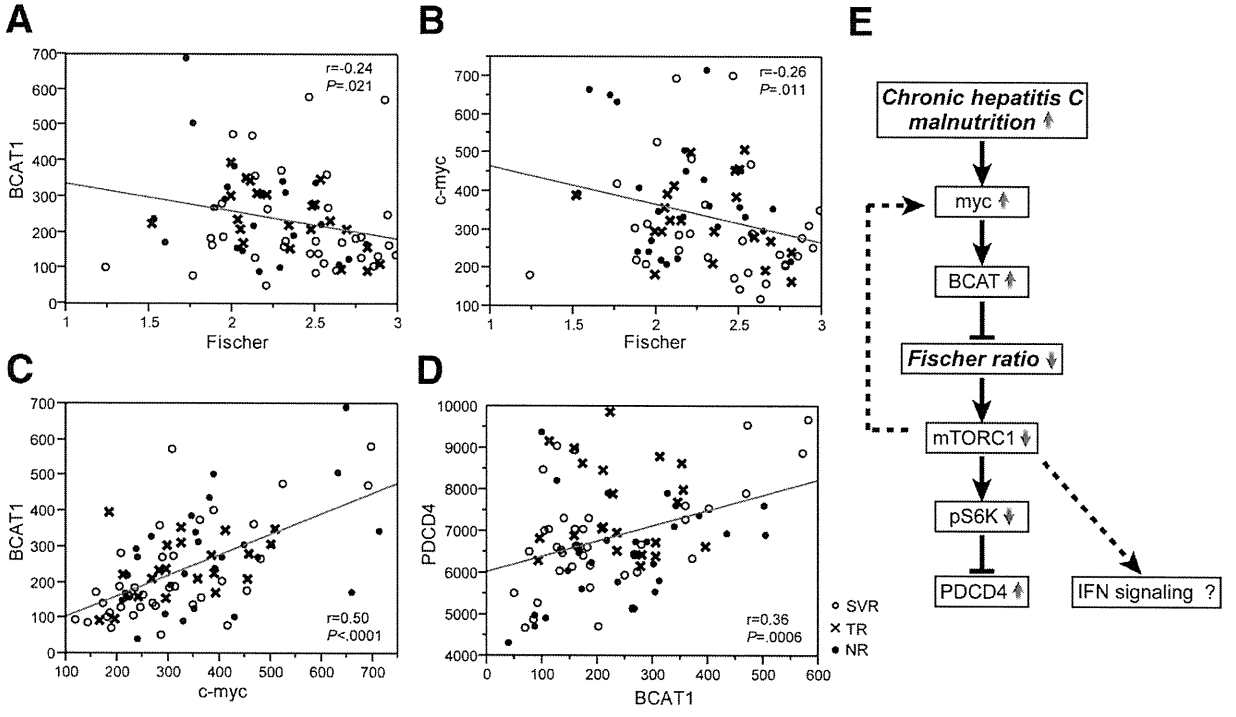

Figure 1. Regression analysis of mTORC1-related gene expression in liver. Gene expression values were determined by probe intensities. (*A*) BCAT1 and Fischer's ratio. (*B*) c-myc and Fischer's ratio. (*C*) BCAT1 and c-myc. (*D*) PDCD4 and BCAT1. (*E*) Putative signaling of mTORC1-related genes in CH-C.

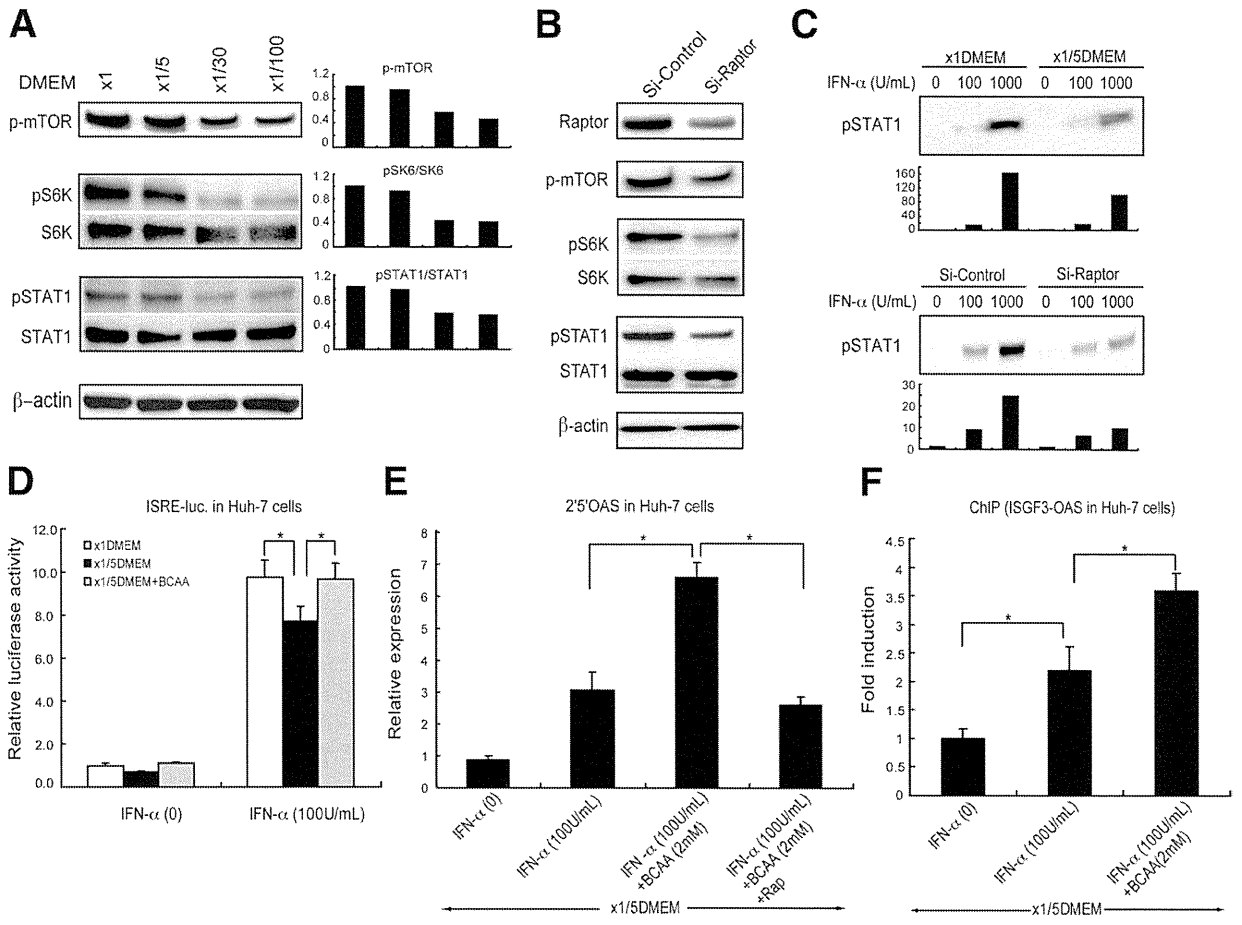

Figure 2. mTORC1 and IFN signaling in Huh-7 cells in low-amino-acid medium. (*A*) p-mTOR, pS6K, and pSTAT1 expression in different amino acid media. (*B*) p-mTOR, pS6K, and pSTAT1 expression under Raptor knock-down conditions. (*C*) IFN-alfa stimulation and pSTAT1 expression in low-amino-acid media or under Raptor knock-down conditions. (*D*) IFN-alfa stimulation and ISRE reporter activities in normal and low-amino-acid media. (*E*) IFN-alfa stimulation and 2'5'OAS expression supplemented with BCAA or rapamycin in low-amino-acid medium. (*F*) Chromatin immunoprecipitation of 2'5'OAS promoter region by ISGF3γ.

The induction of pSTAT1 by IFN-alfa (1000 U/mL) stimulation was impaired in ×1/5 DMEM or in Raptor knocked-down condition, compared with the control (Figure 2*C*). Consistent with these results, IFN-alfa–induced ISRE-dependent transcriptional activity, as measured using an ISRE-luciferase reporter assay, was impaired significantly in ×1/5 DMEM compared with ×1 DMEM (Figure 2*D*). However, this activity could be rescued by the addition of 2 mmol/L BCAA (Figure 2*D*). These results were confirmed by determining the expression of the endogenous IFN-alfa responsive gene, 2'5'OAS, using quantitative reverse-transcription PCR. Figure 2*E* shows that BCAA treatment augmented 2'5'OAS expression in low levels of amino acids, and that this could be reversed by the addition of rapamycin, an inhibitor of mTORC1 (Figure 2*E*). Furthermore, chromatin immunoprecipitation (ChIP) experiments revealed that transcriptional augmentation by BCAA was mediated by the binding of the IFN-alfa–inducible transcription factor, ISGF3γ, to the promoter region of 2'5'OAS (Figure 2*F*). These results indicate that amino acids in culture media play an essential role in IFN-alfa signaling through mTORC1 signaling, and that the addition of BCAA can overcome impaired IFN-alfa signaling in Huh-7 cells.

Induction of Socs3 in Low-Amino-Acid Medium in Huh-7 Cells

Besides being involved in mTOR signaling, Foxo transcriptional factors mediate another important branch of nutrition-sensing signaling pathway.[17] Therefore, we evaluated forkhead box O3A (Foxo3a) expression in low-amino-acid conditions in Huh-7 cells. After 6 hours culture in ×1/5, ×1/30, and ×1/100 DMEM, expression of the phosphorylated form of Foxo3a (pFoxo3a) decreased, whereas that of total Foxo3a increased in ×1/5 and ×1/30 DMEM, and the ratio of pFoxo3a to Foxo3a (pFoxo3a/Foxo3a) substantially decreased (Figure 3*A* and *B*). It has been reported that dephosphorylated Foxo3a is translocated to the nucleus before activation of its target genes.[18] In the present study, immunofluorescent staining

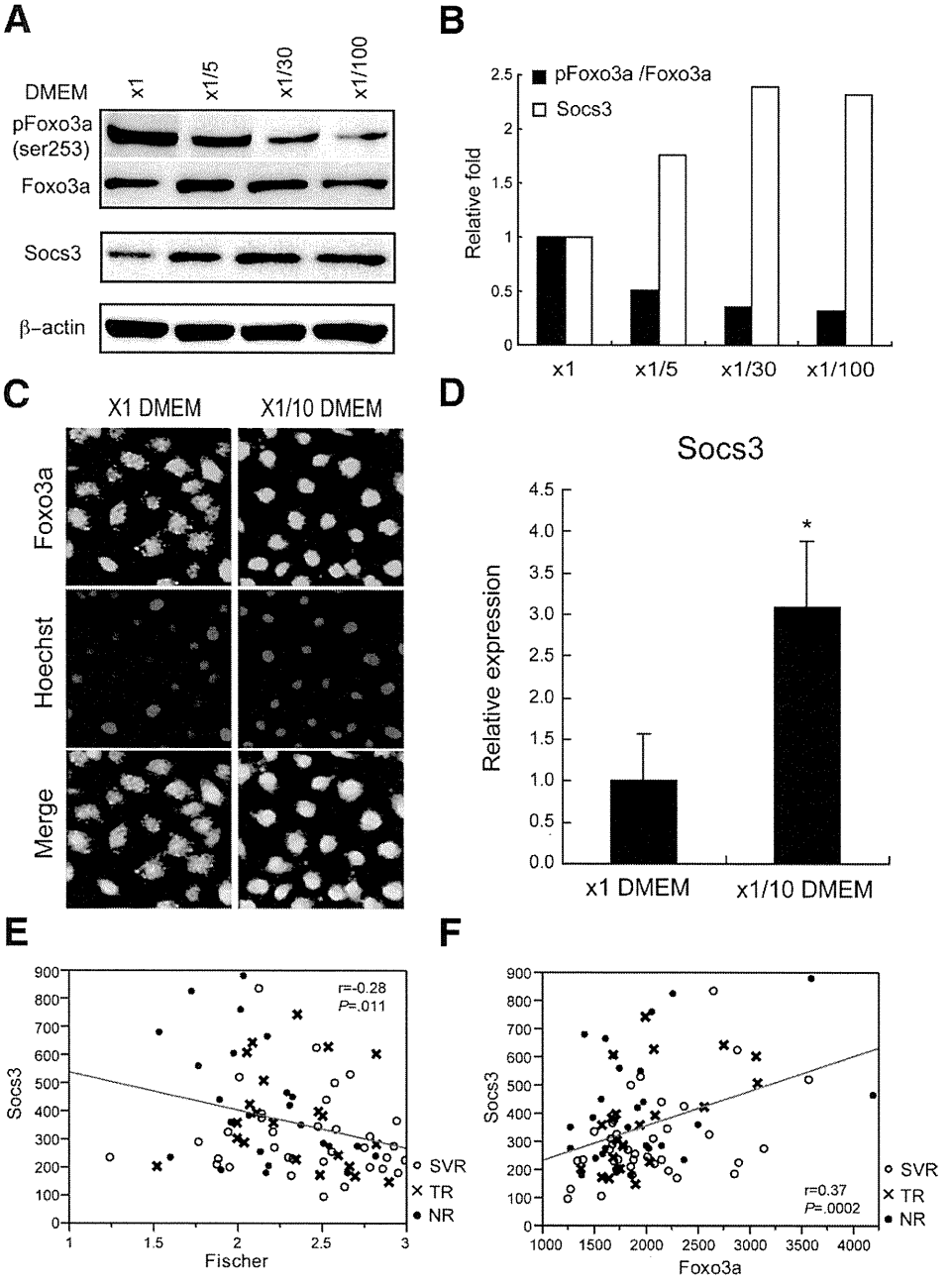

Figure 3. Foxo3a and Socs3 signaling in Huh-7 cells in low-amino-acid medium. (*A*) Foxo3a and Socs3 expression in different amino acid media. (*B*) Relative change of pFoxo3a/Foxo3a and Socs3 expression in different amino acid media. (*C*) Immunofluorescence staining of Foxo3a in Huh-7 cells in normal and low-amino-acid media. (*D*) Relative change of Socs3 messenger RNA in Huh-7 cells in normal and low-amino-acid media. (*E*) Regression analysis of Socs3 in liver and Fischer's ratio. (*F*) Regression analysis of Socs3 and Foxo3a in liver.

with an anti-Foxo3a antibody showed that Foxo3a diffused in both the cytoplasm and nucleus in normal amino acid medium, but localized in the nucleus in low-amino-acid medium (×1/10 DMEM) (Figure 3*C*).

Interestingly, in low-amino-acid medium, transcription and protein expression of Socs3 increased significantly (Figure 3*A*, *B*, and *D*). The induction of Socs3 in a state of malnutrition also was confirmed in clinical samples. In CH-C livers there was a significant negative correlation between the plasma Fischer's ratio and Socs3 expression, implying that Socs3 expression increases during the malnutrition state induced by CH-C. There was also a significant correlation between Foxo3a and the transcriptional level of Socs3 in CH-C livers (Figure 3*E* and *F*), suggesting an in vitro and in vivo biological role for Foxo3a in the activation of Socs3 expression. These findings also were confirmed by Western blotting of CH-C livers (Supplementary Figure 2, Supplementary Table 2).

Socs3 Is a Transcriptional Target of Foxo3a

The significant correlation between Socs3 and Foxo3a in CH-C livers prompted us to analyze the Socs3 promoter sequence and, in doing so, we identified a putative Foxo binding element (FBE) (Figure 4*A*). To investigate the functional relevance of Foxo3a in the transcriptional regulation of Socs3, we constructed reporter plasmids containing a luciferase coding region fused to the Socs3 promoter region (Socs3-luc). Socs3-luc promoter activity was increased substantially by the overexpression of Foxo3a (Figure 4*B*). The mutations introduced in the putative FBE (FBEmut) in the Socs3 promoter significantly reduced Foxo3a-induced Socs3 promoter activation (Figure 4*B*).

Foxo3a then was knocked down by siRNA and Socs3 induction was evaluated. After suppression of Foxo3a (Supplementary Figure 3), Socs3 promoter activity was repressed significantly in low-amino-acid medium (×1/10 DMEM) (Figure 4*C*). Thus, Foxo3a appears to be indispensable for activating the Socs3 promoter under low-amino-acid conditions. Correlating with these results, ChIP assays using an anti-Foxo3a antibody showed a significant increase in the association between Foxo3a and the FBE of the Socs3 promoter in low-amino-acid conditions (×1/10 DMEM) (Figure 4*D*). Taken together, these results suggest that, besides mTORC1 signaling, the Foxo3a-mediated Socs3 signaling pathway might contribute to impaired IFN signaling in a state of malnutrition in CH-C. BCAA potentially restores this signaling (Figure 4*E*).

Effect of BCAA on HCV Replication in Huh-7 or Huh-7.5 Cells

Based on the earlier-described results, we used 2 HCV in vitro replication systems to examine whether BCAA affects HCV replication in Huh-7 or Huh-7.5 cells. The first system used a recombinant infectious genotype 1a clone, H77S.3/GLuc2A (Supplementary Materials and Methods, Supplementary Figure 4), including reporter genes, whereas the second used continuously JFH-1–infecting Huh-7 cells (Supplementary Materials and Methods).

The synthetic RNA transcribed from pH77S.3/GLuc2A was introduced into Huh-7.5 cells and replication of H77S.3/GLuc2A was evaluated in normal or low-amino-acid medium supplemented with BCAA. H77S.3/GLuc2A increased significantly by 2.6-fold in Huh-7.5 cells grown in low-amino-acid medium (×1/5 DMEM) compared with normal amino acid medium (×1 DMEM). Interestingly, BCAA repressed H77S.3/GLuc2A replication in a dose-dependent manner (Figure 5*A*). In agreement with these results, the expression of Mx-1 was increased significantly by the addition of BCAA (Figure 5*B*). Similar findings were observed in JFH-1–infecting Huh-7 cells (Materials and Methods, Supplementary Figure 4). Although no obvious increase in HCV replication was observed in low-amino-acid medium (×1/5 DMEM) compared with normal amino acid medium (×1 DMEM), JFH-1 replication was repressed significantly by the addition of BCAA in a dose-dependent manner (Figure 5*D*). The expression of Mx-1 was increased substantially by the addition of BCAA (Figure 5*E*), suggesting that BCAA significantly repressed HCV replication in cells with either naive or persistent HCV infection. Importantly, there were no significant differences in cell viability between the conditions (Figure 5*C* and *F*).

To validate these findings, signaling pathways in HCV replicating cells were examined (Figure 6*A* and *B*). BCAA increased pS6K in a dose-dependent manner, implying its involvement in the activation of mTORC1 signaling. Related to this, expression of pSTAT1 was shown to be increased and the ratio of pSTAT1 to total STAT1 (pSTAT1/STAT1) increased 2.5- to 3-fold after the addition of BCAA. Thus, BCAA activated mTORC1 and the JAK-STAT signaling pathway in HCV-infected cells. In addition, the expression ratio of pFoxo3a to total Foxo3a (pFoxo3a/Foxo3a) increased 3- to 4-fold, indicating an increase in the cytoplasmic form of Foxo3a that is exposed to proteasome degradation. Concordant with these findings, we observed a decrease in the expression of Socs3. In addition, expression of the HCV core protein decreased as shown in Figure 6*A* and *B*. Thus, these results clearly show that BCAA repressed HCV replication through activation of IFN signaling and repression of Socs3-mediated IFN inhibitory signaling, as proposed in Figure 4*E*.

Discussion

Thompson et al[5] showed that the IL-28B polymorphism, HCV RNA, nationality (Caucasian/Hispanic vs African American), hepatic fibrosis stage, and fasting blood sugar level are all significant variables for achieving SVR in patients infected with genotype 1 HCV. However, the significance of variable factors for treatment response in conjunction with the IL-28B polymorphism has not been evaluated fully. In the present study, in addition to previously examined variables,[4] we included the plasma Fischer's ratio as a nutritional parameter. Multivariate analysis showed that the minor type of IL-28B polymorphism, advanced fibrosis stage, high hepatic ISGs, low Fischer's ratio, and ISDR mutation (≤1) independently contributed to NR (Table 1). Interestingly, among patients of similar fibrosis stage (F3–4), the Fischer's ratio was significantly lower in NR than SVR+TR cases. Therefore, the plasma value of Fischer's ratio was associated with the treatment response that was independent of the IL-28B polymorphism and histologic stage of the liver, although patients with advanced hepatic fibrosis are likely to be nutritionally affected.

As a nutrient sensor signaling pathway, the protein kinase mTOR plays an essential role in maintaining homeostasis and regulates protein synthesis in response to nutrient conditions. mTOR is the catalytic subunit of 2 distinct complexes, mTORC1 and mTORC2. In addition

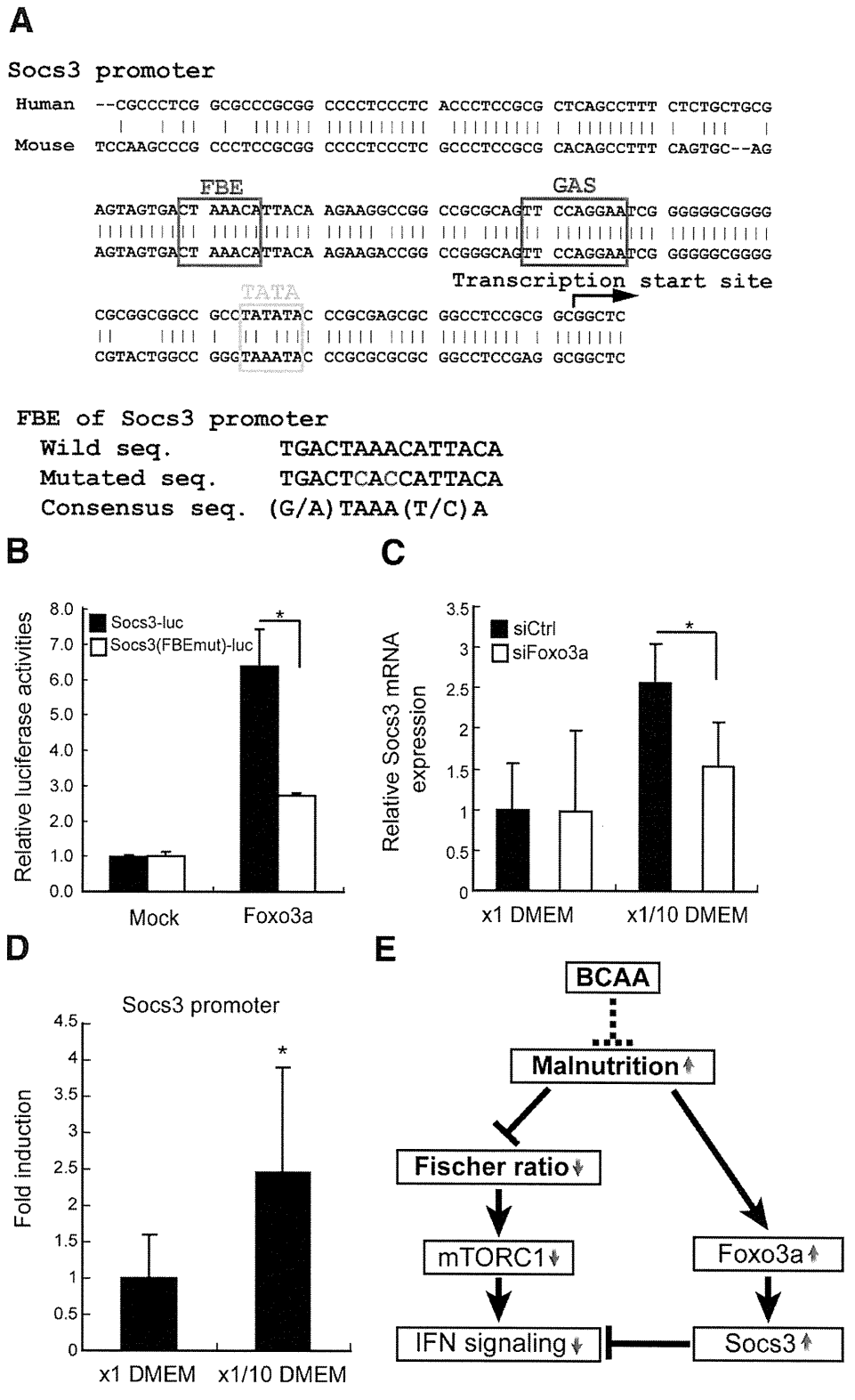

Figure 4. Socs3 promoter assay. (*A*) Primary structure of putative Foxo binding element in Socs3 promoter region. (*B*) Socs3-luc and Socs3 (FBEmut)-luc activities after overexpression of Foxo3a in Huh-7 cells. (*C*) Relative Socs3 messenger RNA (mRNA) expression after knockdown of Foxo3a in normal and low-amino-acid media. (*D*) Chromatin immunoprecipitation of Socs3 promoter region by Foxo3a in normal and low-amino-acid media. (*E*) Model of impaired IFN signaling by repressed mTORC1 signaling and increased Socs3 signaling under CH-C state of malnutrition.

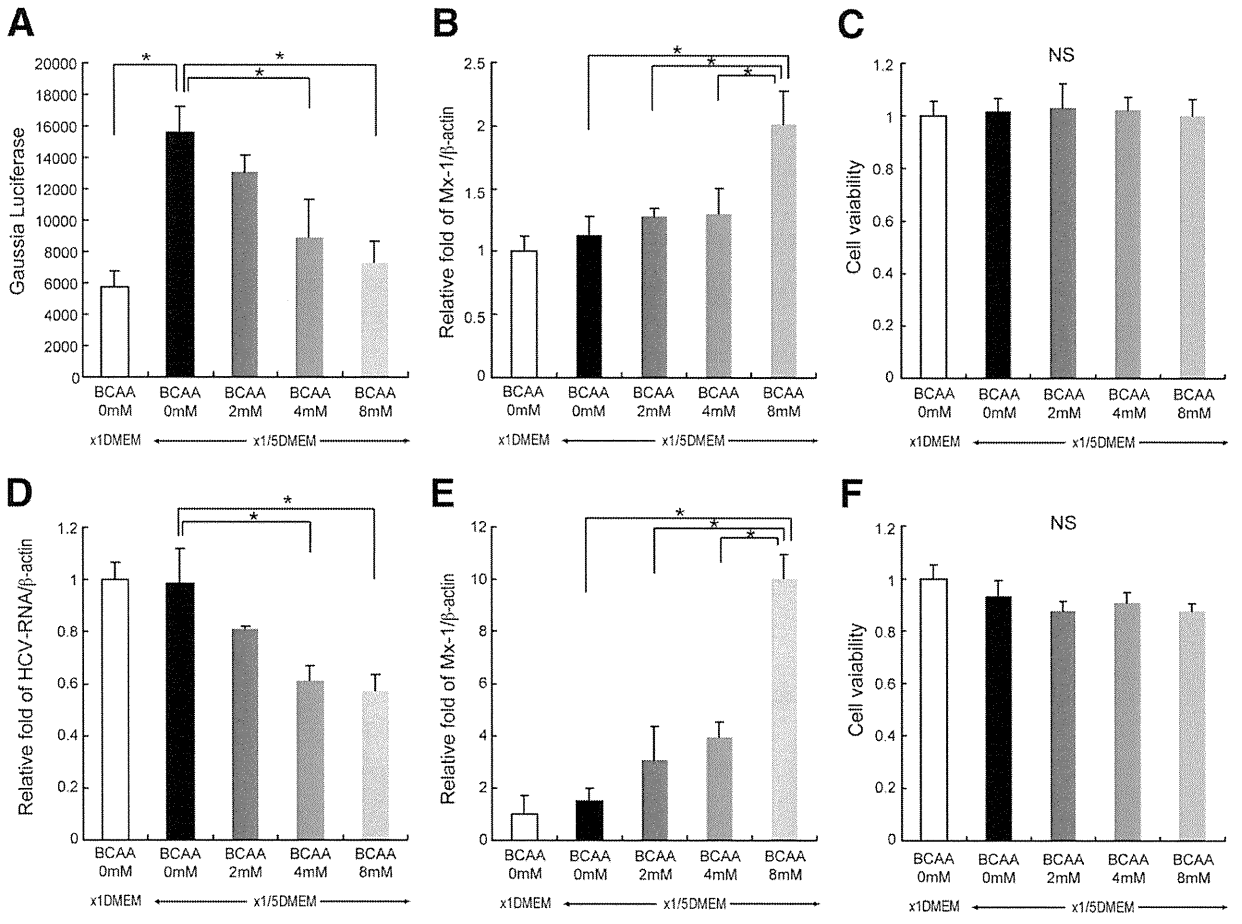

Figure 5. Effect of BCAA on HCV replication in cells in low-amino-acid medium. (*A*) Effect of BCAA on H77S.3/GLuc2A replication in Huh-7.5 cells. (*B*) Mx-1 expression in H77S.3/GLuc2A-transfected Huh-7.5 cells supplemented with BCAA. (*C*) Viability of Huh-7.5 cells. (*D*) Effect of BCAA on JFH-1 replication continuously infecting Huh-7 cells. (*E*) Mx-1 expression in continuously JFH-1–infecting Huh-7 cells supplemented with BCAA. (*F*) Viability of Huh-7 cells.

to these metabolic aspects, recent reports have shown that mTORC1 participates in IFN signaling and antiviral defense responses,[9,10] although the precise signaling pathway has not yet been clarified. In the present study, we evaluated mTORC1 signaling in CH-C livers using gene expression profiling of 91 patients (Figure 1, Supplementary Table 1). We observed a significant negative correlation between plasma Fischer's ratio and hepatic expression of BCAT1, an important catalytic enzyme of BCAA (Figure 1*A*). Moreover, BCAT1 expression was correlated positively with PDCD4 expression, which in turn is regulated negatively by pS6K at the transcriptional level (Figure 1*D*).[16] Thus, the expression of BCAT1 appears to be a negative indicator of mTORC1 signaling in the liver, and the plasma Fischer's ratio is partially reflected by mTORC1 signaling in the liver and muscle.

Interestingly, the expression of c-myc was correlated significantly with BCAT1 (Figure 1*C*) as reported previously.[15] Several studies observed up-regulated c-myc expression in advanced stages of CH-C[19] but, on the other hand, c-myc recently was shown to be a target of mTORC1 in hepatic cells.[17] The existence of a feedback mechanism between c-myc and mTORC1 signaling to maintain liver homeostasis (Figure 1*E*) is plausible, although the precise mechanisms need to be confirmed.

Impaired mTORC1 signaling is suggested to affect the IFN-alfa–induced signaling pathway. To address this, the relationship between mTORC1 and IFN signaling was assessed using a cell culture system. In low-amino-acid medium (×1/5, ×1/30, and ×1/100 DMEM), expression of pSTAT1 was decreased substantially, correlating with the impaired mTORC1 signaling represented by decreased p-mTOR and pS6K expression in Huh-7 cells (Figure 2*A*).

The relationship between mTORC1 and IFN signaling was confirmed further by the knock-down experiment of Raptor, a specific subunit of mTORC1 (Figure 2*B*), although a more precise analysis should be performed to confirm this relationship. Importantly, when Huh-7 cells were stimulated by IFN-alfa, pSTAT1 induction was repressed significantly in low-amino-acid medium (×1/5 DMEM) or in Raptor knocked-down conditions (Figure 2*C*). It therefore could be speculated that IFN treat-

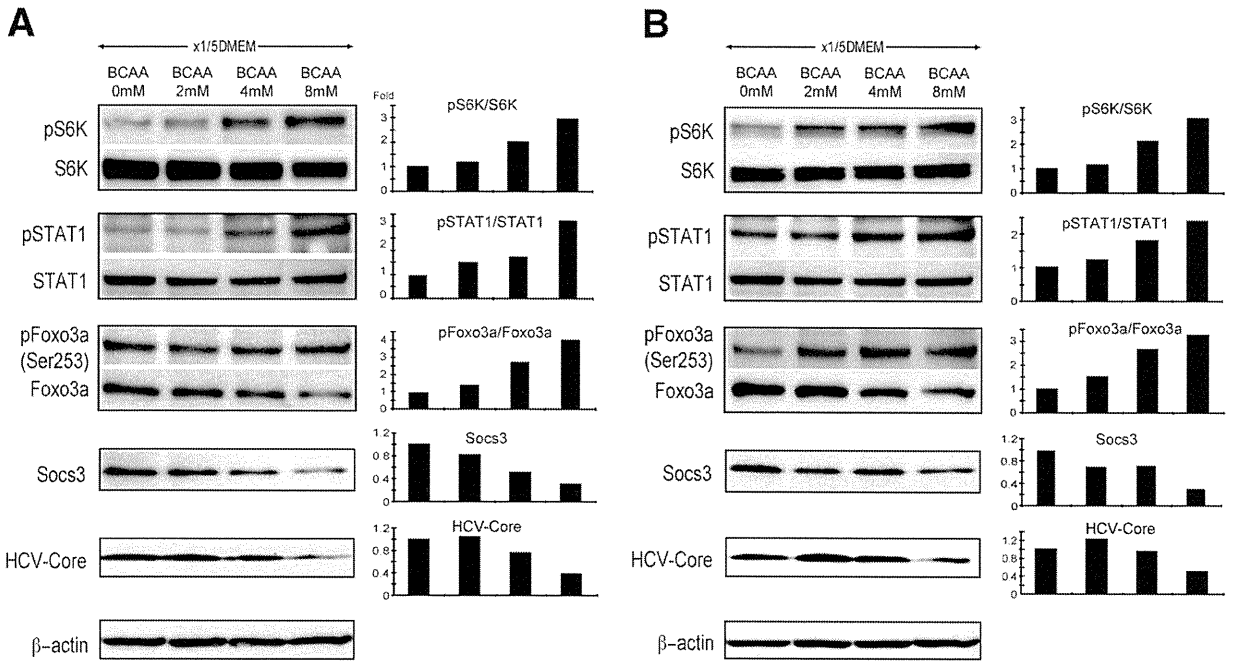

Figure 6. Expression of S6K, STAT1, Foxo3a, Socs3, and HCV core in H77S.3/GLuc2A-transfected Huh-7.5 cells or continuously JFH-1–infecting Huh-7 cells supplemented with BCAA.

ment of patients with liver malnutrition and impaired mTORC1 signaling would lead to reduced induction of ISGs. Importantly, BCAA was able to restore impaired IFN signaling through increased binding of ISGF3γ to its targets (Figure 2*D–F*).

Besides cross-talk of mTORC1 and IFN signaling, we revealed that Foxo3a also is involved in the IFN inhibitory pathway. In low-amino-acid medium, expression of pFoxo3a (ser253) was decreased substantially whereas that of Socs3 was increased. A decreased pFoxo3a/Foxo3a ratio indicates nuclear accumulation of Foxo3a before activation of its target genes, and this was confirmed by immunofluorescent staining (Figure 3*C*). The expression of Foxo3a was significantly positively correlated with that of Socs3 in CH-C liver (Figure 3*F*). These findings prompted us to identify a putative FBE in the Socs3 promoter region (Figure 4*A*). In fact, Socs3 promoter reporter activity was activated by overexpression of Foxo3a, and mutation of FBE impaired Foxo3a-dependent Socs3 promoter activation. Conversely, induction of Socs3 was not observed when expression of Foxo3a was knocked down by siRNA in low-amino-acid medium. Socs3 induction in low-amino-acid medium was owing to increased binding of Foxo3a to the FBE, which was confirmed by ChIP (Figure 4*D*). Therefore, in addition to impaired mTORC1 signaling, the Foxo3a-mediated Socs3 IFN inhibitory pathway might be involved in impaired IFN signaling in patients with liver malnutrition (Figure 4*E*).

Finally, we examined whether BCAA could restore impaired IFN signaling and inhibit HCV replication in cells under conditions of malnutrition. Importantly, BCAA could repress replication of the recombinant genotype 1a-derived HCV, H77S.3/GLuc2A, in a dose-dependent manner (Figure 5*A*). H77S.3/GLuc2A RNA produces infectious virus[14] and, therefore, the results indicate that BCAA might act on a naive HCV infection. Moreover, BCAA inhibited JFH-1–infected Huh-7 cells in which JFH-1 continuously was infecting in a dose-dependent manner. These results indicate that BCAA had an inhibitory effect on either naive or persistent HCV infection irrespective of genotypes (1a and 2a). Consistent with these results, BCAA induced the expression of pSTAT1 and Mx protein in a dose-dependent manner, and repressed Socs3 expression through increasing the ratio of pFoxo3a (ser243) to Foxo3a in a dose-dependent manner (Figures 5 and 6). Therefore, BCAA potentially could restore impaired IFN signaling and inhibit HCV replication in a CH-C state of malnutrition.

In conclusion, we addressed the clinical significance of the nutritional state of the liver on the treatment response of Peg-IFN and RBV combination therapy for CH-C. Although further studies are required to fully define the precise mechanisms underlying mTOR and IFN signaling, we showed that plasma values of Fischer's ratio are a useful nutritional parameter associated with treatment response. Fischer's ratio reflects mTORC1 signaling in the liver, which is correlated with IFN signaling and related to Socs3 IFN inhibitory signaling through Foxo3a. The potential usefulness of BCAA for the augmentation of IFN signaling could suggest a new therapeutic application for advanced-stage CH-C.

Supplementary Material

Note: To access the supplementary material accompanying this article, visit the online version of *Gastroenterology* at www.gastrojournal.org, and at doi: 10.1053/j.gastro.2011.03.051.

Appendix A

The Hokuriku Liver Study Group is composed of the following members: Drs Takashi Kagaya, Kuniaki Arai, Kaheita Kakinoki, Kazunori Kawaguchi, Hajime Takatori, and Hajime Sunakosaka (Department of Gastroenterology, Kanazawa University Graduate School of Medicine, Kanazawa, Japan); Drs Touru Nakahama and Shinji Kamiyamamoto (Kurobe City Hospital, Kurobe, Toyama, Japan); Dr Yasuhiro Takemori (Toyama Rosai Hospital, Uozu, Toyama, Japan); Dr Hikaru Oguri (Koseiren Namerikawa Hospital, Namerikawa, Toyama, Japan); Drs Yatsugi Noda and Hidero Ogino (Toyama Prefectural Central Hospital, Toyama, Japan); Drs Yoshinobu Hinoue and Keiji Minouchi (Toyama City Hospital, Toyama, Japan); Dr Nobuyuki Hirai (Koseiren Takaoka Hospital, Takaoka, Toyama, Japan); Drs Tatsuho Sugimoto and Koji Adachi (Tonami General Hospital, Tonam, Toyama, Japan); Dr Yuichi Nakamura (Noto General Hospital, Nanao, Ishikawa, Japan); Drs Masashi Unoura and Ryuhei Nishino (Public Hakui Hospital, Hakui, Ishikawa, Japan); Drs Hideo Morimoto and Hajime Ohta (National Hospital Organization Kanazawa Medical Center, Kanazawa, Ishikawa, Japan); Dr Hirokazu Tsuji (Kanazawa Municipal Hospital, Kanazawa, Ishikawa, Japan); Drs Akira Iwata and Shuichi Terasaki (Kanazawa Red Cross Hospital, Kanazawa, Ishikawa, Japan); Drs Tokio Wakabayashi and Yukihiro Shirota (Saiseikai Kanazawa Hospital, Kanazawa, Ishikawa, Japan); Drs Takeshi Urabe and Hiroshi Kawai (Public Central Hospital of Matto Ishikawa, Hakusan, Ishikawa, Japan); Dr Yasutsugu Mizuno (Nomi Municipal Hospital, Nomi, Ishikawa, Japan); Dr Shoni Kameda (Komatsu Municipal Hospital, Komatsu Ishikawa, Japan); Drs Hirotoshi Miyamori and Uichiro Fuchizaki (Keiju Medical Center, Nanao, Ishikawa, Japan); Dr Haruhiko Shyugo (Kanazawa Arimatsu Hospital, Kanazawa, Ishikawa, Japan); Dr Hideki Osaka (Yawata Medical Center, Komatsu, Ishikawa, Japan); Dr Eiki Matsushita (Kahoku Central Hospital, Tsubata, Ishikawa, Japan); Dr Yasuhiro Katou (Katou Hospital, Komatsu, Ishikawa, Japan); Drs Nobuyoshi Tanaka and Kazuo Notsumata (Fukuiken Saiseikai Hospital, Fukui, Japan); Dr Mikio Kumagai (Kumagai Clinic, Tsuruga, Fukui, Japan); and Dr Manabu Yoneshima (Municipal Tsuruga Hospital, Tsuruga, Fukui, Japan).

References

1. Fried MW, Shiffman ML, Reddy KR, et al. Peginterferon alfa-2a plus ribavirin for chronic hepatitis C virus infection. N Engl J Med 2002;347:975–982.
2. Tanaka Y, Nishida N, Sugiyama M, et al. Genome-wide association of IL28B with response to pegylated interferon-alpha and ribavirin therapy for chronic hepatitis C. Nat Genet 2009;41: 1105–1109.
3. Ge D, Fellay J, Thompson AJ, et al. Genetic variation in IL28B predicts hepatitis C treatment-induced viral clearance. Nature 2009;461:399–401.
4. Honda M, Sakai A, Yamashita T, et al. Hepatic ISG expression is associated with genetic variation in interleukin 28B and the outcome of IFN therapy for chronic hepatitis C. Gastroenterology 2010;139:499–509.
5. Thompson AJ, Muir AJ, Sulkowski MS, et al. Interleukin-28B polymorphism improves viral kinetics and is the strongest pretreatment predictor of sustained virologic response in genotype 1 hepatitis C virus. Gastroenterology 2010;139:120–129 e18.
6. Nishitani S, Ijichi C, Takehana K, et al. Pharmacological activities of branched-chain amino acids: specificity of tissue and signal transduction. Biochem Biophys Res Commun 2004;313:387–389.
7. Matsumura T, Morinaga Y, Fujitani S, et al. Oral administration of branched-chain amino acids activates the mTOR signal in cirrhotic rat liver. Hepatol Res 2005;33:27–32.
8. Kim DH, Sarbassov DD, Ali SM, et al. mTOR interacts with raptor to form a nutrient-sensitive complex that signals to the cell growth machinery. Cell 2002;110:163–175.
9. Colina R, Costa-Mattioli M, Dowling RJ, et al. Translational control of the innate immune response through IRF-7. Nature 2008;452: 323–328.
10. Kaur S, Lal L, Sassano A, et al. Regulatory effects of mammalian target of rapamycin-activated pathways in type I and II interferon signaling. J Biol Chem 2007;282:1757–1768.
11. Shimbo K, Kubo S, Harada Y, et al. Automated precolumn derivatization system for analyzing physiological amino acids by liquid chromatography/mass spectrometry. Biomed Chromatogr 2009; 24:683–691.
12. Shirasaki T, Honda M, Mizuno H, et al. La protein required for internal ribosome entry site-directed translation is a potential therapeutic target for hepatitis C virus replication. J Infect Dis 2010;202:75–85.
13. Yi M, Villanueva RA, Thomas DL, et al. Production of infectious genotype 1a hepatitis C virus (Hutchinson strain) in cultured human hepatoma cells. Proc Natl Acad Sci U S A 2006;103:2310–2315.
14. Shimakami T, Welsch C, Yamane D, et al. Protease inhibitor-resistant hepatitis C virus mutants with reduced fitness from impaired production of infectious virus. Gastroenterology 2011; 140:667–675.
15. Eden A, Simchen G, Benvenisty N. Two yeast homologs of ECA39, a target for c-Myc regulation, code for cytosolic and mitochondrial branched-chain amino acid aminotransferases. J Biol Chem 1996; 271:20242–2045.
16. Dowling RJ, Topisirovic I, Alain T, et al. mTORC1-mediated cell proliferation, but not cell growth, controlled by the 4E-BPs. Science 2010;328:1172–1176.
17. Teleman AA, Hietakangas V, Sayadian AC, et al. Nutritional control of protein biosynthetic capacity by insulin via Myc in Drosophila. Cell Metab 2008;7:21–32.
18. Zhang X, Gan L, Pan H, et al. Phosphorylation of serine 256 suppresses transactivation by FKHR (FOXO1) by multiple mechanisms. Direct and indirect effects on nuclear/cytoplasmic shuttling and DNA binding. J Biol Chem 2002;277: 45276–45284.
19. Farinati F, Cardin R, Bortolami M, et al. Oxidative damage, pro-inflammatory cytokines, TGF-alpha and c-myc in chronic HCV-related hepatitis and cirrhosis. World J Gastroenterol 2006;12: 2065–2069.

Received October 19, 2010. Accepted March 18, 2011.

Reprint requests

Address requests for reprints to: Shuchi Kaneko, MD, PhD, Department of Gastroenterology, Graduate School of Medicine, Kanazawa University, Takara-Machi 13-1, Kanazawa 920-8641, Japan. e-mail: skaneko@m-kanazawa.jp; e-mail: fax: (81) 76-234-4250.

Acknowledgments

Participating investigators from the Hokuriku Liver Study Group are listed in Appendix A.

The authors thank Mina Nishiyama and Yuki Hatayama for excellent technical assistance.

Conflicts of interest

The authors disclose no conflicts.

Supplementary Materials and Methods

Plasma Amino Acid Analysis

Plasma sample amino acid concentrations were measured by high-performance liquid chromatography-electrospray ionization-mass spectrometry followed by derivatization.[1] An MSQ Plus LC/MS system (Thermo Fischer Scientific, Waltham, MA) equipped with an electrospray ionization source was used in positive ionization mode for selected ion monitoring. Xcalibur version 1.4 SR1 software (Thermo Fischer Scientific, Yokohama, Japan) was used for data collection and processing. The high-performance liquid chromatography separation system consisted of an L-2100 pump, L-2200 autosampler, and L-2300 column oven (Hitachi High-Technologies Corporation, Tokyo, Japan). A Wakosil-II 3C8-100HG column (100, 2.1, 3 mm; Wako Pure Chemical Industries, Osaka, Japan) was used for the separation, and the mobile phase consisted of eluent A (25-mmol/L ammonium formate in water, pH 6.0) and eluent B (water:acetonitrile = 40:60).

Western Blotting

The expression of HCV core protein, Socs3, Foxo3a, phospho-Foxo3a (Ser253) (pFoxo3a), STAT1, pSTAT1 (Tyr701), S6K, pS6K, p-mTOR (Ser2448), Raptor, and β-actin were evaluated with mouse anti-core (Affinity BioReagents, Golden, CO), mouse anti-Socs3 (Santa Cruz Biotechnology, Santa Cruz, CA), rabbit anti-Foxo3a, rabbit anti-β-actin (Sigma-Aldrich, St Louis, MO), rabbit anti-phospho-Foxo3a (Ser253), rabbit anti-STAT1, rabbit anti-p-STAT1 (Tyr701), rabbit anti-p70 S6K, rabbit anti-pS6K, rabbit anti-p-mTOR (Ser2448), and rabbit anti-Raptor (Cell Signaling Technology, Beverly, MA), respectively. Densitometric analysis was conducted directly on the blotted membrane using a charge coupled device camera system (LAS-3000 Mini; Fujifilm, Tokyo, Japan) and Scion Image software (Frederick, MD).

Primer Sequences for PCR and siRNA

Primer sequences for PCR and siRNA were as follows: 2′5′OAS: forward 5′- CTC AGA AAT ACC CCA GCC AAA TC-3′, reverse 5′-GTG GTG AGA GGA CTG AGG AA-3′; Socs3: forward 5′-TAC CAC CTG AGT CTC CAG CTT CTC-3′, reverse 5′-CCT GGC AGT TCT CAT TAG TTC AGC ATT C-3′; Foxo3a: forward 5′-TGC TGT ATG CAA GAA CTT TCC AGT AGC AG-3′, reverse 5′-ACT CTA GCC CCC ATG CTA CTA GTG-3′; glyceraldehyde-3-phosphate dehydrogenase: forward 5′-GAA GGT GAA GGT CGG AGT-3′, reverse 5′-GAA GAT GGT GAT GGG ATT TC-3′, siFoxo3a (SASI_Hs01_00119127; Sigma) sense: 5′-GAA UGA UGG GCU GAC UGA AdTdT-3′, antisense: 5′-UUC AGU CAG CCC AUC AUU CdTdT-3′. Small interfering Raptor was purchased as part of KIAA1303 siGENOME SMART pool siRNA reagents from Dharmacon, Inc (Lafayette, CO).

Construction of ISRE-Luc Reporter and FBEmut-luc Reporter Plasmids

Oligonucleotides containing the ISRE tandem repeat sequence (sense 5′-TCG AGA ACT GAA ACT GAA ACT GAA ACT GAA ACT GAA ACT GAA ACT GAA ACT GAA ACT GAA A-3′, antisense 5′-AGC TTT TCA GTT TCA GTT TCA GTT TCA GTT TCA GTT TCA GTT TCA GTT TCA GTT TCA GTT C-3′, consensus 5′-GAA Ann GAA ACT-3′) were annealed, and integrated into Xho I and Hind III sites of the pGL4.23 luciferase vector (Promega). The human Socs3 promoter region (-109/+217) was amplified by genomic PCR using specific primers (forward, 5′-TGC TGC GAG TAG TGA CTA AAC ATT ACA AG-3′ and reverse, 5′-CCG TGA AGT CCA CAA AGG AGC CTT C-3′) and cloned into the EcoR V site of the pGL4.10-luc2 reporter vector (Promega). The Socs3 FBE mutant reporter vector was created by substituting 2 adenines in the putative FBE with guanines (wild-type sequence 5′-CTAAACA-3′, mutated sequence 5′-CTGAGCA-3′).

ChIP Assay

For the ChIP assay using the anti-ISGF3γ antibody, 1×10^6 Huh-7 cells were treated with IFN-alfa (0 or 100 U/mL) and BCAA (2 mmol/L) in low-amino-acid medium for 6 hours. For ChIP using the anti-Foxo3a antibody, 1×10^6 Huh-7 cells were cultured in low-amino-acid medium for 24 hours.

Cells were cross-linked with 1% formaldehyde in PBS for 10 minutes at 37°C, and the reaction was stopped with 250 mmol/L glycine for 10 minutes. Cells were suspended in sodium dodecyl sulfate-lysis buffer (1% sodium dodecyl sulfate, 10 mmol/L ethylenediaminetetraacetic acid [EDTA], 50 mmol/L Tris-HCl [pH 8.1]), complete protease inhibitor cocktail (Roche Applied Science), and incubated for 30 minutes at 10°C. Cell lysate was sonicated with Bioruptor (Cosmo Bio, Tokyo, Japan) to obtain chromatin fragments and diluted 10-fold in ChIP dilution buffer (0.01% sodium dodecyl sulfate, 1.1% Triton-X 100, 1.2 mmol/L EDTA, 16.7 mmol/L Tris-HCl [pH 8.1], 150 mmol/L NaCl, complete protease inhibitor cocktail). Chromatin fragments were incubated with 2 μg ISGF3γ antibody (Santa Cruz Biotechnology), 2 μg Foxo3a antibody (H-144; Santa Cruz Biotechnology), or normal rabbit immunoglobulin G for 18 hours at 4°C. Dynabeads (30 μL) protein G (Invitrogen) was added and incubated for 1 hour at 4°C. The beads were washed with low-salt-wash buffer (0.1% sodium dodecyl sulfate, 1% Triton-X 100, 2.0 mmol/L EDTA, 20 mmol/L Tris-HCl [pH 8.1], 150 mmol/L NaCl), high-salt-wash buffer (0.1% sodium dodecyl sulfate, 1% Triton-X 100, 2.0 mmol/L EDTA, 20 mmol/L Tris-HCl [pH 8.1], 500 mmol/L NaCl), LiCl wash buffer (250 mmol/L LiCl, 1% NP-40, 1% de-

oxycholate, 1.0 mmol/L EDTA, 1.0 mmol/L Tris-HCl [pH 8.1]) and Tris-EDTA buffer. Immunoprecipitated chromatin fragments were eluted with elution buffer (1% sodium dodecyl sulfate, 100 mmol/L NaHCO3, 10 mmol/L dithiothreitol), and reverse cross-linked by incubating for 6 hours at 65°C in elution buffer containing 200 mmol/L NaCl. DNA fragments were purified and quantified by real-time detection PCR with primers for putative ISRE in the 2′5′OAS promoter region (forward, 5′-AAA TGC ATT TCC AGA GCA GAG TTC AGA G-3′, reverse, 5′-GGG TAT TTC TGA GAT CCA TCA TTG ACA GG-3′) or putative FBE in the Socs3 promoter region (forward, 5′-TGC TGC GAG TAG TGA CTA AAC ATT ACA AG -3′, reverse, 5′-AGC GGA GCA GGG AGT CCA AGT C -3′). Values were normalized by the measurement of input DNA.

pH77S.3/GLuc2A

pH77S.2 is a modification of pH77S[2] containing an additional mutation within the E2 protein (N476D in the polyprotein) that promotes infectious virus yields from RNA-transfected cells (Yi et al, unpublished data). To monitor replication, the GLuc sequence, fused at its C terminus to the foot-and-mouth disease virus 2A autoprotease, was inserted between p7 and NS2 of pH77S.2 (Supplementary Figure 4). To insert the GLuc-coding sequence between p7 and NS2 in pH77S.2, followed by the foot-and-mouth disease virus 2A protein-coding sequence, Mlu I, EcoR V, and Spe I restriction sites were created between the p7 and NS2 coding sequences by site-directed mutagenesis. DNA coding for GLuc was subcloned into the Mlu I and EcoR V sites of the modified plasmid after PCR amplification using the primers: 5′- ATA ATA TTA CGC GTA *TGG GAG TCA AAG TTC TGT TTG CC*-3′ (sequence corresponding to the N-terminal GLuc is italicized and that corresponding to Mlu I is underlined) and 5′-ATA AAT AGAT ATC *GTC ACC ACC GGC CCC CTT GAT CTT*-3′ (C terminal GLuc is italicized and EcoR V is underlined). A DNA fragment encoding the 17 amino acids of the foot-and-mouth disease virus 2A protein was generated by annealing the following complementary oligonucleotides: 5′- ATA TGA TAT CAA CTT TGA CCT TCT CAA GTT GGC CGG CGA CGT CGA GTC CAA CCC AGG GCC CAC TAG CAT AT-3′ and 5′-ATA TGC TAG TGG GCC CTG GGT TGG ACT CGA CGT CGC CGG CCA ACT TGA GAA GGT CAA AGT TGA TAT CAT AT-3′ (underlined sequences indicate EcoR V and Spe I sites). The annealed oligonucleotides were digested by both restriction enzymes and the product inserted into the corresponding sites of pH77S.2 containing GLuc to generate pH77S.2/GLuc2A. Q41R is a cell-culture adaptive mutation within the NS3 protease domain of pH77S. Because it is not essential for production of infectious virus (Yi et al, unpublished data), pH77S.2 and pH77S.2/GLuc2A constructs underwent this mutation by site-directed mutagenesis of a PCR fragment spanning the Afe I and BsrG I sites to replace Gln_{41} with wild-type Arg. The resulting plasmids (pH77S.2/R41Q and pH77S.2/GLuc2A/R41Q) were redesignated pH77S.3 and pH77S.3/GLuc2A, respectively.[3,4] GLuc has several advantages over other luciferase reporter enzymes in that it is smaller and allows more sensitive detection than either firefly or Renilla luciferase.[3,4] In addition, a signal sequence directs its secretion into cell-culture media, allowing real-time dynamic measurements of GLuc expression without the need for cell lysis. H77S.3/GLuc2A RNA produces infectious virus, although with lower efficiency than H77S.3 RNA (10-fold less).

References

1. Shimbo K, Kubo S, Harada Y, et al. Automated precolumn derivatization system for analyzing physiological amino acids by liquid chromatography/mass spectrometry. Biomed Chromatogr 2009; 24:683–691.
2. Yi M, Villanueva RA, Thomas DL, et al. Production of infectious genotype 1a hepatitis C virus (Hutchinson strain) in cultured human hepatoma cells. Proc Natl Acad Sci U S A 2006;103:2310–2315.
3. Shetty S, Kim S, Shimakami T, et al. Hepatitis C virus genomic RNA dimerization is mediated via a kissing complex intermediate. RNA 2010;16:913–925.
4. Shimakami T, Welsch C, Yamane D, et al. Protease inhibitor-resistant hepatitis C virus mutants with reduced fitness from impaired production of infectious virus. Gastroenterology 2011; 140:667–675.

Research Article

EASL EUROPEAN ASSOCIATION FOR THE STUDY OF THE LIVER | JOURNAL OF HEPATOLOGY

Pre-treatment prediction of response to pegylated-interferon plus ribavirin for chronic hepatitis C using genetic polymorphism in *IL28B* and viral factors

Masayuki Kurosaki[1], Yasuhito Tanaka[2], Nao Nishida[3], Naoya Sakamoto[4], Nobuyuki Enomoto[5], Masao Honda[6], Masaya Sugiyama[2], Kentaro Matsuura[2], Fuminaka Sugauchi[2], Yasuhiro Asahina[1], Mina Nakagawa[4], Mamoru Watanabe[4], Minoru Sakamoto[5], Shinya Maekawa[5], Akito Sakai[6], Shuichi Kaneko[6], Kiyoaki Ito[7], Naohiko Masaki[7], Katsushi Tokunaga[3], Namiki Izumi[1,*], Masashi Mizokami[2,7]

[1]*Division of Gastroenterology and Hepatology, Musashino Red Cross Hospital, Tokyo, Japan;* [2]*Department of Virology, Liver Unit, Nagoya City University, Graduate School of Medical Sciences, Nagoya, Japan;* [3]*Department of Human Genetics, Graduate School of Medicine, University of Tokyo, Tokyo, Japan;* [4]*Department of Gastroenterology and Hepatology, Tokyo Medical and Dental University, Tokyo, Japan;* [5]*First Department of Internal Medicine, University of Yamanashi, Yamanashi, Japan;* [6]*Department of Gastroenterology, Kanazawa University, Graduate School of Medicine, Kanazawa, Japan;* [7]*Research Center for Hepatitis and Immunology, International Medical Center of Japan, Konodai Hospital, Ichikawa, Japan*

Background & Aims: Pegylated interferon and ribavirin (PEG-IFN/RBV) therapy for chronic hepatitis C virus (HCV) genotype 1 infection is effective in 50% of patients. Recent studies revealed an association between the *IL28B* genotype and treatment response. We aimed to develop a model for the pre-treatment prediction of response using host and viral factors.

Methods: Data were collected from 496 patients with HCV genotype 1 treated with PEG-IFN/RBV at five hospitals and universities in Japan. *IL28B* genotype and mutations in the core and IFN sensitivity determining region (ISDR) of HCV were analyzed to predict response to therapy. The decision model was generated by data mining analysis.

Results: The *IL28B* polymorphism correlated with early virological response and predicted null virological response (NVR) (odds ratio = 20.83, p <0.0001) and sustained virological response (SVR) (odds ratio = 7.41, p <0.0001) independent of other covariates. Mutations in the ISDR predicted relapse and SVR independent of *IL28B*. The decision model revealed that patients with the minor *IL28B* allele and low platelet counts had the highest NVR (84%) and lowest SVR (7%), whereas those with the major *IL28B* allele and mutations in the ISDR or high platelet counts had the lowest NVR (0–17%) and highest SVR (61–90%). The model had high reproducibility and predicted SVR with 78% specificity and 70% sensitivity.

Conclusions: The *IL28B* polymorphism and mutations in the ISDR of HCV were significant pre-treatment predictors of response to PEG-IFN/RBV. The decision model, including these host and viral factors may support selection of optimum treatment strategy for individual patients.

Keywords: *IL28B*; ISDR; Peg-interferon; Ribavirin; Data mining; Decision tree.
Received 14 March 2010; received in revised form 22 June 2010; accepted 7 July 2010; available online 19 September 2010

* Corresponding author. Address: Division of Gastroenterology and Hepatology, Musashino Red Cross Hospital, 1-26-1 Kyonan-cho, Musashino-shi, Tokyo 180-8610, Japan. Tel.: +81 422 32 3111; fax: +81 422 32 9551.
E-mail address: nizumi@musashino.jrc.or.jp (N. Izumi).

Introduction

Hepatitis C virus (HCV) infection is the leading cause of cirrhosis and hepatocellular carcinoma worldwide [1]. The successful eradication of HCV, defined as a sustained virological response (SVR), is associated with a reduced risk of developing hepatocellular carcinoma. Currently, pegylated interferon (PEG-IFN) plus ribavirin (RBV) is the most effective standard of care for chronic hepatitis C but the rate of SVR is around 50% in patients with HCV genotype 1 [2,3], the most common genotype in Japan, Europe, the United States, and many other countries. Moreover, 20–30% of patients with HCV genotype 1 have a null virological response (NVR) to PEG-IFN/RBV therapy [4]. The most reliable method for predicting the response is to monitor the early decline of serum HCV-RNA levels during treatment [5] but there is no established method for prediction before treatment. Because PEG-IFN/RBV therapy is costly and often accompanied by adverse effects such as flu-like symptoms, depression and hematological abnormalities, pre-treatment predictions of those patients who are unlikely to benefit from this regimen enables ineffective treatment to be avoided.

Recently, it has been reported through a genome-wide association study (GWAS) of patients with genotype 1 HCV that single nucleotide polymorphisms (SNPs) located near the *IL28B* gene are strongly associated with a response to PEG-IFN/RBV therapy in

ELSEVIER

Journal of Hepatology **2011** vol. 54 | 439–448

Table 1. Baseline characteristics of all patients, and patients assigned to the model building or validation groups.

	All patients n = 496	Model group n = 331	Validation group n = 165
Gender: male	250 (50%)	170 (51%)	80 (48%)
Age (years)	57.1 ± 9.9	56.8 ± 9.7	57.5 ± 10.2
ALT (IU/L)	78.6 ± 60.8	78.1 ± 61.4	79.7 ± 59.6
GGT (IU/L)	59.3 ± 63.6	58.9 ± 62.0	60.2 ± 66.9
Platelets (10^9/L)	154 ± 53	153 ± 52	154 ± 56
Fibrosis: F3-4	121 (24%)	80 (24%)	41 (25%)
HCV-RNA: >600,000 IU/ml	409 (82%)	273 (82%)	136 (82%)
ISDR mutation: ≤1	220 (88%)	290 (88%)	145 (88%)
Core 70 (Arg/Gln or His)	293 (59%)/203 (41%)	197 (60%)/134 (40%)	96 (58%)/69 (42%)
Core 91 (Leu/Met)	299 (60%)/197 (40%)	200 (60%)/131 (40%)	99 (60%)/66 (40%)
IL28B: Minor allele	151 (30%)	101 (31%)	50 (30%)
SVR	194 (39%)	129 (39%)	65 (39%)
Relapse	152 (31%)	103 (31%)	49 (30%)
NVR	150 (30%)	99 (30%)	51 (31%)

ALT, alanine aminotransferase; GGT, gamma-glutamyltransferase; ISDR, interferon sensitivity determining region; Arg, arginine; Gln, glutamine; His, histidine; Leu, leucine; Met, methionine; Minor, heterozygote or homozygote of minor allele; SVR, sustained virological response; NVR, null virological response.

Japanese [6], European [7], and a multi-ethnic population [8,9]. The last three studies focused on the association of SNPs in the *IL28B* region with SVR [7–9] but we found a stronger association with NVR [6]. In addition to these host genetic factors, we have reported that mutations within a stretch of 40 amino acids in the NS5A region of HCV, designated as the IFN sensitivity determining region (ISDR), are closely associated with the virological response to IFN therapy: a lower number of mutations is associated with treatment failure [10–13]. Amino acid substitutions at positions 70 and 91 of the HCV core region (Core70, Core91) also have been reported to be associated with response to PEG-IFN/RBV therapy: glutamine (Gln) or histidine (His) at Core70 and methionine (Met) at Core91 are associated with treatment resistance [4,14]. The importance of substitutions in the HCV core and ISDR was confirmed recently by a Japanese multicenter study [15]. How these viral factors contribute to response to therapy is yet to be determined. For general application in clinical practice, host genetic factors and viral factors should be considered together.

Data mining analysis is a family of non-parametric regression methods for predictive modeling. Software is used to automatically explore the data to search for optimal split variables and to build a decision tree structure [16]. The major advantage of decision tree analysis over logistic regression analysis is that the results of the analysis are presented in the form of flow chart, which can be interpreted intuitively and readily made available for use in clinical practice [17]. The decision tree analysis has been utilized to define prognostic factors in various diseases [18–25]. We have reported recently its usefulness for the prediction of an early virological response (undetectable HCV-RNA within 12 weeks of therapy) to PEG-IFN/RBV therapy in chronic hepatitis C [26].

This study aimed to define the pre-treatment prediction of response to PEG-IFN/RBV therapy through the integrated analysis of host factors, such as the *IL28B* genetic polymorphism and various clinical covariates, as well as viral factors, such as mutations in the HCV core and ISDR and serum HCV-RNA load. In addition, for the general application of these results in clinical practice, decision models for the pre-treatment prediction of response were determined by data mining analysis.

Materials and methods

Patients

This was a multicentre retrospective study supported by the Japanese Ministry of Health, Labor and Welfare. Data were collected from a total of 496 chronic hepatitis C patients who were treated with PEG-IFN alpha and RBV at five hospitals and universities throughout Japan. Of these, 98 patients also were included in the original GWAS analysis [6]. The inclusion criteria in this study were as follows (1) infection by genotype 1b, (2) lack of co-infection with hepatitis B virus or human immunodeficiency virus, (3) lack of other causes of liver disease, such as autoimmune hepatitis, and primary biliary cirrhosis, (4) completion of at least 24 weeks of therapy, (5) adherence of more than 80% to the planned dose of PEG-IFN and RBV for the NVR patients, (6) availability of DNA for the analysis of the genetic polymorphism of *IL28B*, and (7) availability of serum for the determination of mutations in the ISDR and substitutions of Core70 and Core91 of HCV. Patients received PEG-IFN alpha-2a (180 μg) or 2b (1.5 μg/kg) subcutaneously every week and were administered a weight adjusted dose of RBV (600 mg for <60 kg, 800 mg for 60–80 kg, and 1000 mg for >80 kg daily) which is the recommended dosage in Japan. Written informed consent was obtained from each patient and the study protocol conformed to the ethical guidelines of the Declaration of Helsinki and was approved by the institutional ethics review committee. The baseline characteristics are listed in Table 1. For the data mining analysis, 67% of the patients (331 patients) were assigned randomly to the model building group and 33% (165 patients) to the validation group. There were no significant differences in the clinical backgrounds between these two groups.

Laboratory and histological tests

Blood samples were obtained before therapy and were analyzed for hematologic tests and for blood chemistry and HCV-RNA. Sequences of ISDR and the core region of HCV were determined by direct sequencing after amplification by reverse-transcription and polymerase chain reaction as reported previously [4,11]. Genetic polymorphism in one tagging SNP located near the *IL28B* gene (rs8099917) was determined by the GWAS or DigiTag2 assay [27]. Homozygosity (GG) or heterozygosity (TG) of the minor sequence was defined as having the *IL28B* minor allele, whereas homozygosity for the major sequence (TT) was

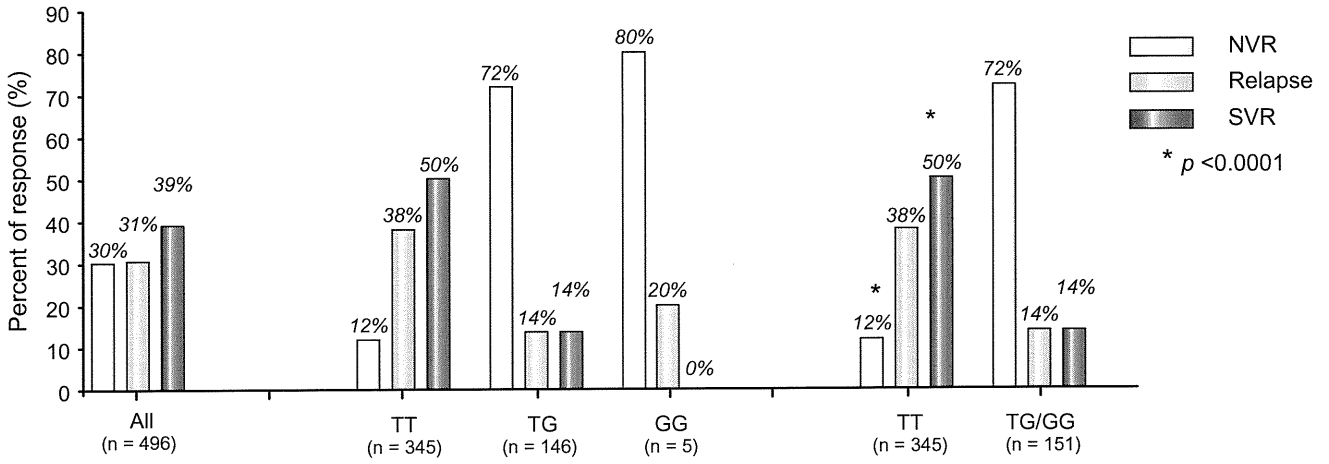

Fig. 1. Association between the IL28B genotype (rs8099917) and treatment response. The rates of response to treatment are shown for each rs8099917 genotype. The rate of null virological response (NVR), relapse, and sustained virological response (SVR) is shown. The *p* values are from Fisher's exact test. The rate of NVR was significantly higher (p <0.0001) and the rate of SVR was significantly lower (p <0.0001) in patients with the *IL28B* minor allele compared to those with the major allele.

defined as having the *IL28B* major allele. In this study, NVR was defined as a less than 2 log reduction of HCV-RNA at week 12 and detectable HCV-RNA by qualitative PCR with a lower detection limit of 50 IU/ml (Amplicor, Roche Diagnostic systems, CA) at week 24 during therapy. RVR (rapid virological response) and complete early virological response (cEVR) were defined as undetectable HCV-RNA at 4 weeks and 12 weeks during therapy and SVR was defined as undetectable HCV-RNA 24 weeks after the completion of therapy. Relapse was defined as reappearance of HCV-RNA after the completion of therapy. The stage of liver fibrosis was scored according to the METAVIR scoring system: F0 (no fibrosis), F1 (mild fibrosis: portal fibrosis without septa), F2 (moderate fibrosis: few septa), F3 (severe fibrosis: numerous septa without cirrhosis) and F4 (cirrhosis). Percentage of steatosis was quantified in 111 patients by determining the average proportion of hepatocytes affected by steatosis.

Statistical analysis

Associations between pre-treatment variables and treatment response were analyzed by univariate and multivariate logistic regression analysis. Associations between the *IL28B* polymorphism and sequences of HCV were analyzed by Fisher's exact test. SPSS software v.15.0 (SPSS Inc., Chicago, IL) was used for these analyses. For the data mining analysis, IBM-SPSS Modeler version 13.0 (IBM-SPSS Inc., Chicago, IL) software was utilized as reported previously [26]. The patients used for model building were divided into two groups at each step of the analysis based on split variables. Each value of each variable was considered as a potential split. The optimum variables and cut-off values were determined by a statistical search algorithm to generate the most significant division into two prognostic subgroups that were as homogeneous as possible for the probability of SVR. Thereafter, each subgroup was evaluated again and divided further into subgroups. This procedure was repeated until no additional significant variable was detected or the sample size was below 15. To avoid over-fitting, 10-fold cross validation was used in the tree building process. The reproducibility of the resulting model was tested with the data from the validation patients.

Results

Association between the IL28B (rs8099917) genotype and the PEG-IFN/RBV response

The rs8099917 allele frequency was 70% for TT (n = 345), 29% for TG (n = 146), and 1% for GG (n = 5). We defined the *IL28B* major allele as homozygous for the major sequence (TT) and the *IL28B* minor allele as homozygous (GG) or heterozygous (TG) for the minor sequence. The rate of NVR was significantly higher (72% vs. 12%, p <0.0001) and the rate of SVR was significantly lower (14% vs. 50%, p <0.0001) in patients with the *IL28B* minor allele compared to those with the major allele (Fig. 1).

Effect of the IL28B polymorphism, substitutions in the ISDR, Core70, and Core91 of HCV on time-dependent clearance of HCV

Patients were stratified according to their *IL28B* allele type, the number of mutations in the ISDR, the amino acid substitutions in Core70 and Core91, and the rate of undetectable HCV-RNA at 4, 8, 12, 24, and 48 weeks after the start of therapy were analyzed (Fig. 2A–D). The rate of undetectable HCV-RNA was significantly higher in patients with the *IL28B* major allele than the minor allele, in patients with two or more mutations in the ISDR compared to none or only one mutation, in patients with arginine (Arg) at Core70 rather than Gln/His, and in patients with leucine (Leu) at Core91 rather than Met. The difference was most significant when stratified by the *IL28B* allele type. The rate of RVR and cEVR was significantly more frequent in patients with the *IL28B* major allele compared with those with the *IL28B* minor allele: 9% vs. 3% for RVR (p <0.005) and 57% vs. 11% for cEVR (p <0.0001). These findings suggest that *IL28B* has the greatest impact on early virological response to therapy.

Association between substitutions in the ISDR and relapse after the completion of therapy

Patients were stratified according to the *IL28B* allele, number of mutations in the ISDR, and amino acid substitutions of Core70 and Core91, and the rate of relapse was analyzed (Fig. 3A and B). Among patients who achieved cEVR, the rate of relapse was significantly lower in patients with two or more mutations in the ISDR compared to those with only one or no mutations (15% vs. 31%, p <0.005) (Fig. 3 B). On the other hand, the relapse rate was not different between the *IL28B* major and minor alleles within patients who achieved RVR (3% vs. 0%) or cEVR (28% vs. 29%) (Fig. 3A). Amino acid substitutions of Core70 and Core91 were not associated with the rate of relapse (data not shown).

Factors associated with response by multivariate logistic regression analysis

By univariate analysis, the minor allele of *IL28B* (p <0.0001), one or no mutations in the ISDR (p = 0.03), high serum level of

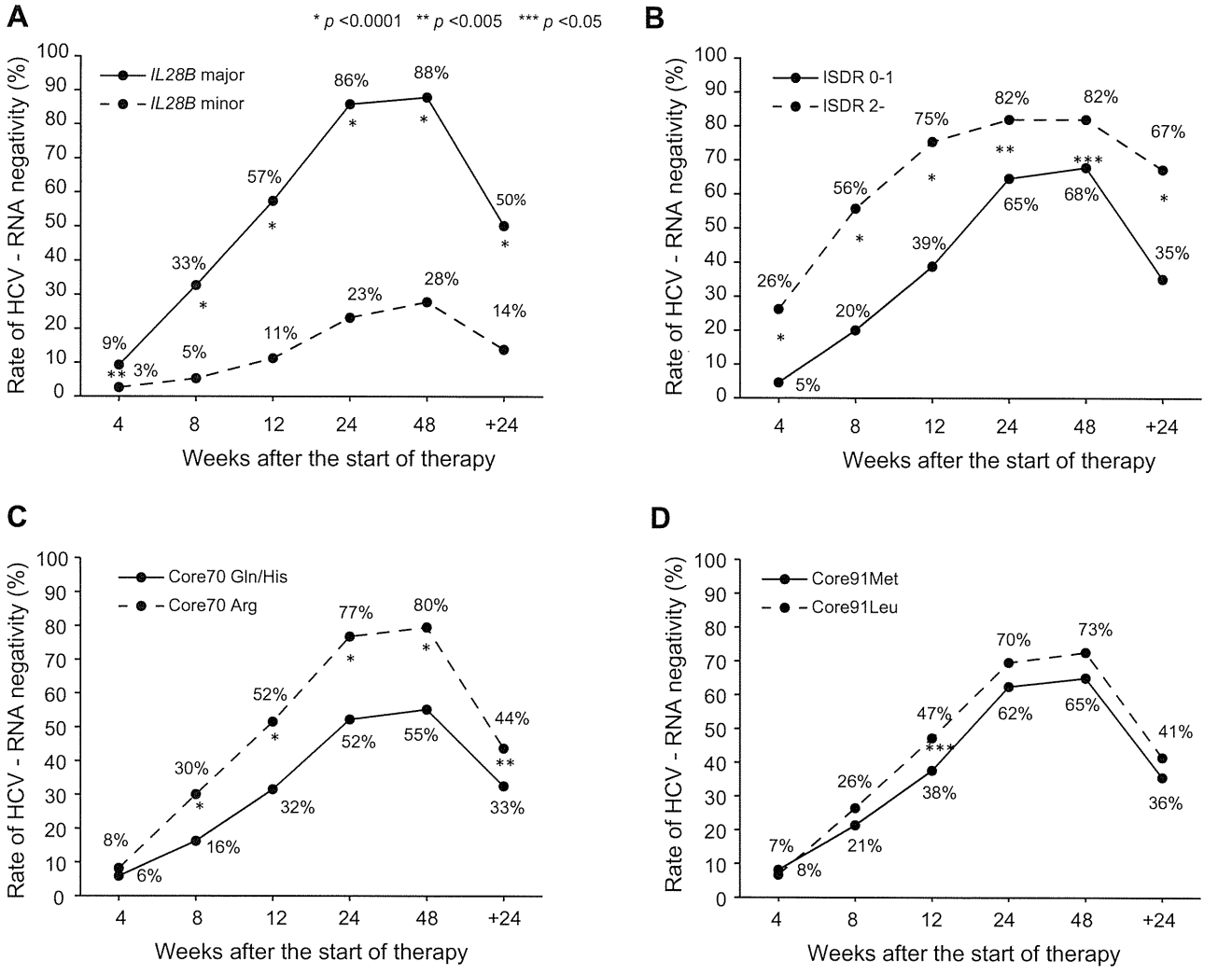

Fig. 2. Effect of *IL28B* mutations in the ISDR, Core70, and Core91 of HCV on time-dependent clearance of HCV. The rate of undetectable HCV-RNA was plotted for serial time points after the start of therapy (4, 8, 12, 24, and 48 weeks) and for 24 weeks after the completion of therapy. Patients were stratified according to (A) the *IL28B* allele (minor allele vs. major allele), (B) the number of mutations in the ISDR (0–1 mutation vs. 2 or more mutations), amino acid substitutions of (C) Core70 (Gln/His vs. Arg), and (D) Core91 (Met vs. Leu). The *p* values are from Fisher's exact test.

HCV-RNA ($p = 0.035$), Gln or His at Core70 ($p < 0.0001$), low platelet counts ($p = 0.009$), and advanced fibrosis ($p = 0.0002$) were associated with NVR. By multivariate analysis, the minor allele of *IL28B* (OR = 20.83, 95%CI = 11.63–37.04, $p < 0.0001$) was associated with NVR independent of other covariates (Table 2). Notably, mutations in the ISDR ($p = 0.707$) and at amino acid Core70 ($p = 0.207$) were not significant in multivariate analysis due to the positive correlation with the *IL28B* polymorphism ($p = 0.004$ for ISDR and $p < 0.0001$ for Core70, Fig. 4).

Genetic polymorphism of *IL28B* also was associated with SVR (OR = 7.41, 95% CI = 4.05–13.57, $p < 0.0001$) independent of other covariates, such as platelet counts, fibrosis, and serum levels of HCV-RNA. Mutation in the ISDR was an independent predictor of SVR (OR = 2.11, 95% CI = 1.06–4.18, $p = 0.033$) but the amino acid at Core70 was not (Table 3).

Factors associated with the IL28B polymorphism

Patients with the *IL28B* minor allele had significantly higher serum level of gamma-glutamyltransferase (GGT) and a higher frequency of hepatic steatosis (Table 4). When the association between the *IL28B* polymorphism and HCV sequences was analyzed, Gln or His at Core70, that is linked to resistance to PEG-IFN and RBV therapy [4,14,15], was significantly more frequent in patients with the minor *IL28B* allele than in those with the major allele (67% vs. 30%, $p < 0.0001$) (Fig. 4). Other HCV sequences with an IFN resistant phenotype also were more prevalent in patients with the minor *IL28B* allele than those with the major allele: Met at Core91 (46% vs. 37%, $p = 0.047$) and one or no mutations in the ISDR (94% vs. 85%, $p = 0.004$) (Fig. 4).

Data mining analysis

Data mining analysis was performed to build a model for the prediction of SVR and the result is shown in Fig. 5. The analysis selected four predictive variables, resulting in six subgroups of patients. Genetic polymorphism of *IL28B* was selected as the best predictor of SVR. Patients with the minor *IL28B* allele had a lower probability of SVR and a higher probability of NVR than those with the major *IL28B* allele (SVR: 14% vs. 50%, NVR: 72% vs.

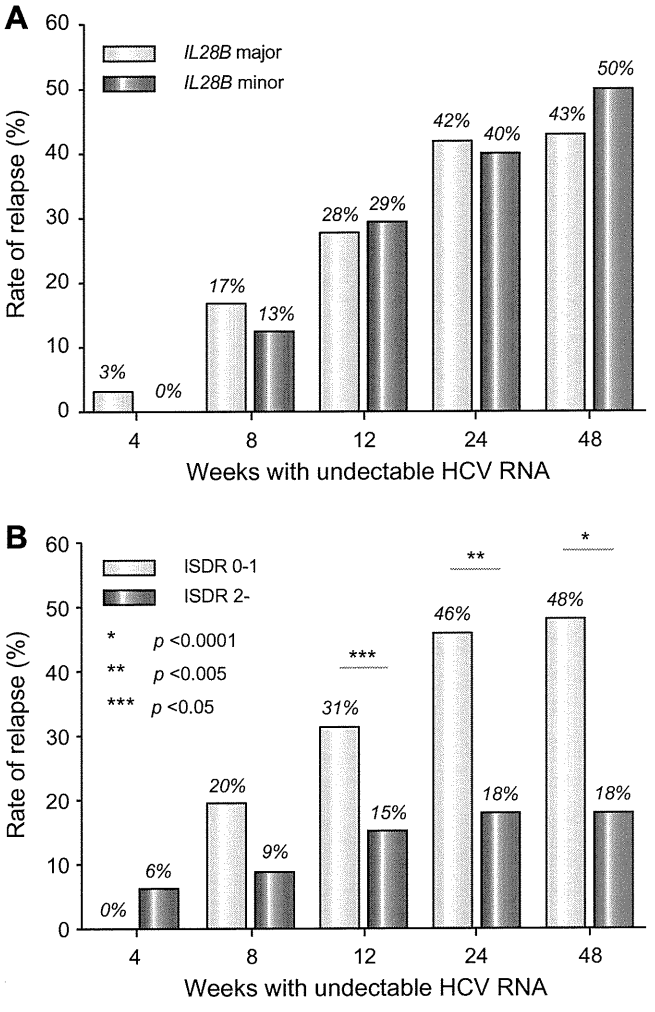

Fig. 3. Association between relapse and the *IL28B* allele or mutations in the ISDR. The rate of relapse was calculated for patients who had undetectable HCV-RNA at serial time points after the start of therapy (4, 8, 12, 24, and 48 weeks). Patients were stratified according to (A) the *IL28B* allele (minor allele vs. major allele) and (B) the number of mutations in the ISDR (0–1 mutation vs. 2 or more mutations). The *p* values are from Fisher's exact test.

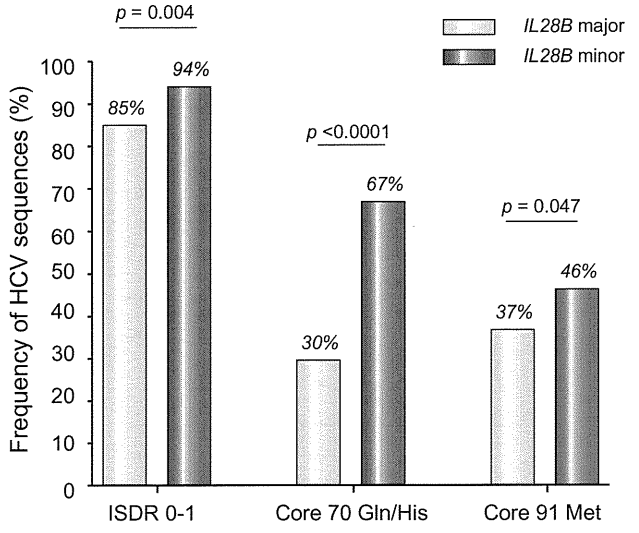

Fig. 4. Associations between the *IL28B* allele and HCV sequences. The prevalence of HCV sequences predicting a resistant phenotype to IFN was higher in patients with the minor *IL28B* allele than those with major allele. (A) 0 or 1 mutation in the ISDR of NS5A, (B) Gln or His at Core70, and (C) Met at Core91. *p* values are from Fisher's exact test.

12%). After stratification by the *IL28B* allele, patients with low platelet counts (<140 × 10^9/L) had a lower probability of SVR and higher probability of NVR than those with high platelet counts (⩾140 × 10^9/L): for the minor *IL28B* allele, SVR was 7% vs. 19%, and NVR was 84% vs. 62%, and for the major *IL28B* allele, SVR was 32% vs. 66% and NVR was 16% vs. 8%. Among patients with the major *IL28B* allele and low platelet counts, those with two or more mutations in the ISDR had a higher probability of SVR and lower probability of relapse than those with one or no mutations in the ISDR (SVR: 75% vs. 27%, and relapse: 8% vs. 57%). Among patients with the major *IL28B* allele and high platelet counts, those with a low HCV-RNA titer (<600,000 IU/ml) had a higher probability of SVR and lower probability of NVR and relapse than those with a high HCV-RNA titer (SVR: 90% vs. 61%, NVR: 0% vs. 10%, and relapse: 10% vs. 29%). The sensitivity and specificity of the decision tree were 78% and 70%, respectively. The area under the receiver operating characteristic (ROC) curve of the model was 0.782 (data not shown). The proportion of patients with advanced fibrosis (F3-4) was 39% (84/217) in patients with low platelet counts (<140 × 10^9/L) compared to 13% (37/279) in those with high platelet counts (⩾140 × 10^9/L).

Validation of the data mining analysis

The results of the data mining analysis were validated with 165 patients who differed from those used for model building. Each patient was allocated to one of the six subgroups for the validation using the flow-chart form of the decision tree. The rate of SVR and NVR in each subgroup was calculated. The rates of SVR and NVR for each subgroup of patients were closely correlated between the model building and the validation patients (r^2 = 0.99 and 0.98) (Fig. 6).

Discussion

The rate of NVR after 48 weeks of PEG-IFN/RBV therapy among patients infected with HCV of genotype 1 is around 20–30%. Previously, there have been no reliable baseline predictors of NVR or SVR. Because more potent therapies, such as protease and polymerase inhibitor of HCV [28,29] and nitazoxianide [30], are in clinical trials and may become available in the near future, a pre-treatment prediction of the likelihood of response may be helpful for patients and physicians, to support clinical decisions about whether to begin the current standard of care or whether to wait for emerging therapies. This study revealed that the *IL28B* polymorphism was the overwhelming predictor of NVR and is independent of host factors and viral sequences reported previously. The *IL28B* encodes a protein also known as IFN-lambda 3, which is thought to suppress the replication of various viruses including HCV [31,32]. The results of the current study and the findings of the GWAS studies [6–9] may provide the rationale for developing diagnostic testing or an IFN-lambda based therapy for chronic hepatitis C in the future.

Table 2. Factors associated with NVR analyzed by univariate and multivariate logistic regression analysis.

	Univariate			Multivariate		
	Odds ratio	95%CI	*p* value	Odds ratio	95%CI	*p* value
Gender: female	0.98	0.67-1.45	0.938	1.29	0.75-2.23	0.363
Age	1.01	0.97-1.01	0.223	0.99	0.97-1.02	0.679
ALT	1.00	1.00-1.00	0.867	1.00	0.99-1.00	0.580
GGT	1.004	1.00-1.01	0.029	1.00	1.00-1.00	0.715
Platelets	0.95	0.91-0.99	0.009	0.92	0.87-0.98	0.006
Fibrosis: F3-4	2.23	1.46-3.42	0.0002	1.97	1.09-3.57	0.025
HCV-RNA: ≥600,000 IU/ml	1.83	1.05-3.19	0.035	2.49	1.17-5.29	0.018
ISDR mutation: ≤1	2.14	1.08-4.22	0.030	0.96	0.78-1.18	0.707
Core 70 (Gln/His)	3.23	2.16-4.78	<0.0001	1.41	0.83-2.42	0.207
Core 91 (Met)	1.39	0.95-2.06	0.093	1.21	0.72-2.04	0.462
IL28B: Minor allele	19.24	11.87-31.18	<0.0001	20.83	11.63-37.04	<0.0001

ALT, alanine aminotransferase; GGT, gamma-glutamyltransferase; ISDR, interferon sensitivity determining region; Gln, glutamine; His, histidine; Met, methionine; Minor allele, heterozygote or homozygote of minor allele.

Table 3. Factors associated with SVR analyzed by univariate and multivariate logistic regression analysis.

	Univariate			Multivariate		
	Odds ratio	95%CI	*p* value	Odds ratio	95%CI	*p* value
Gender: female	0.81	0.56-1.16	0.253	0.86	0.55-1.35	0.508
Age	0.97	0.95-0.99	0.0003	0.99	0.96-1.01	0.199
ALT	1.00	1.00-1.00	0.337	1.00	1.00-1.01	0.108
GGT	1.00	1.00-1.00	0.273	1.00	1.00-1.00	0.797
Platelets	1.12	1.01-116	<0.0001	1.13	1.08-1.19	<0.0001
Fibrosis: F0-2	2.64	1.65-4.22	<0.0001	1.87	1.07-3.28	0.029
HCV-RNA: <600,000 IU/ml	2.49	1.55-3.98	0.0001	2.75	1.55-4.90	0.001
ISDR mutation: 2≤	3.78	2.14-6.68	<0.0001	2.11	1.06-4.18	0.033
Core 70 (Arg)	1.61	1.11-2.28	0.012	0.84	0.52-1.35	0.470
Core 91 (Leu)	1.28	0.88-1.85	0.185	1.26	0.81-1.96	0.300
IL28B: Major allele	6.21	3.75-10.31	<0.0001	7.41	4.05-13.57	<0.0001

ALT, alanine aminotransferase; GGT, Gamma-glutamyltransferase; ISDR, interferon sensitivity determining region; Arg, arginine; Leu, leucine; Major allele, homozygote of major allele.

Among baseline factors, *IL28B* was the most significant predictor of NVR and SVR. Moreover, the *IL28B* allele type was also correlated with early virological response: the rate of RVR and cEVR was significantly high for the *IL28B* major allele compared to the *IL28B* minor allele: 9% vs. 3% for RVR and 57% vs. 11% for cEVR (Fig. 2). On the other hand, the relapse rate was not different between the *IL28B* genotypes within patients who achieved RVR or cEVR (Fig. 3). We believe that optimal therapy should be based on baseline features and a response-guided approach. Our findings suggest that the *IL28B* genotype is a useful baseline predictor of virological response which should be used for selecting the treatment regimen: whether to treat patients with PEG-IFN and RBV or to wait for more effective future therapy including direct acting antiviral drugs. On the other hand, baseline *IL28B* genotype might not be suitable for determining the treatment duration in patients who started PEG-IFN/RBV therapy and whose virological response is determined because the *IL28B* genotype is not useful for the prediction of relapse. The duration of therapy should be personalized based on the virological response. Future studies need to explore whether the combination of baseline *IL28B* genotype and response-guided approach further improves the optimization of treatment duration.

The SVR rate in patients having the *IL28B* minor allele was 14% in the present study while it was 23% in Caucasians and 9% in African Americans in a study by McCarthy et al. [33]. On the other hand, the SVR rate in patients having the *IL28B* minor allele was 28% in genotypes 1/4 compared to 80% in genotypes 2/3 in a study by Rauch et al. [9]. These data imply that the impact of the *IL28B* polymorphism on response to therapy may be different in terms of race, geographical areas, or HCV genotypes, and that our data need to be validated in future studies including different populations and geographical areas before generalization.